Published for SISSA by Springer

Received: October 28, 2018
Revised: February 8, 2019
Accepted: April 3, 2019
Published: April 17, 2019

Search for nonresonant Higgs boson pair production in the $\mathrm{b\bar{b}b\bar{b}}$ final state at $\sqrt{s} = 13\,\mathrm{TeV}$

The CMS collaboration

E-mail: cms-publication-committee-chair@cern.ch

Abstract: Results of a search for nonresonant production of Higgs boson pairs, with each Higgs boson decaying to a $\mathrm{b\bar{b}}$ pair, are presented. This search uses data from proton-proton collisions at a centre-of-mass energy of 13 TeV, corresponding to an integrated luminosity of $35.9\,\mathrm{fb}^{-1}$, collected by the CMS detector at the LHC. No signal is observed, and a 95% confidence level upper limit of 847 fb is set on the cross section for standard model nonresonant Higgs boson pair production times the squared branching fraction of the Higgs boson decay to a $\mathrm{b\bar{b}}$ pair. The same signature is studied, and upper limits are set, in the context of models of physics beyond the standard model that predict modified couplings of the Higgs boson.

Keywords: Beyond Standard Model, Hadron-Hadron scattering (experiments), Higgs physics

ArXiv ePrint: 1810.11854

https://doi.org/10.1007/JHEP04(2019)112

Contents

JHEP04(2019)112

1 Introduction

The detailed understanding of the properties of the Higgs boson (H) discovered in 2012 by the CERN LHC experiments [1–3] remains an important subject in fundamental physics. Current determinations of the properties of the new particle by the ATLAS and CMS Collaborations are found to be in agreement with standard model (SM) predictions [4, 5]. However, there are still many measurements that could reveal unexpected deviations from the SM. A number of models of physics beyond the SM (BSM) can be tested using their predictions of the properties of the observed state, including the Higgs boson self-coupling and couplings to bosons and fermions [6–10].

The production of Higgs boson pairs (HH) is the most direct way to access the Higgs boson self-coupling [11] and to study in detail the SM Higgs potential. The HH production cross section predicted by the SM for 13 TeV proton-proton (pp) collisions and $m_{\mathrm{H}} = 125.09\,\mathrm{GeV}$ [5, 12] is $33.49^{+4.3\%}_{-6.0\%}(\mathrm{scale}) \pm 2.3\%(\alpha_S) \pm 2.1\%(\mathrm{PDF})\,\mathrm{fb}$ [13–17], where the uncertainty is due to the variation of the renormalization (μ_{R}) and factorization (μ_{F}) scales (scale), the strong coupling constant (α_S) uncertainties, and the uncertainty in parton distribution functions (PDF). The predicted cross section results in a low expected event rate, and the acceptance for HH events in the detector is small. This means that the SM HH production process cannot be observed with the data collected so far at the LHC: the expectation is that it will only be possible to set an upper limit on the HH production cross section, as discussed, e.g. in refs. [18, 19]. However, the cross section can be enhanced by anomalous couplings in BSM models [20] and in some cases the enhancement is large enough that HH production could be observed with the current data.

The first searches for nonresonant HH production were performed by LHC experiments using pp collisions data at $\sqrt{s} = 8\,\mathrm{TeV}$ [21, 22]. The data collected in 2015 and 2016 at $\sqrt{s} = 13\,\mathrm{TeV}$ were used for improved analyses in the decay channels: $\mathrm{b\bar{b}b\bar{b}}$ [19], $\mathrm{b\bar{b}}\ell\nu\ell\nu$ [23], $\mathrm{b\bar{b}}\ell\nu\mathrm{qq}$ [24], $\mathrm{b\bar{b}}\tau\tau$ [18, 25], $\mathrm{b\bar{b}}\gamma\gamma$ [26, 27], $\gamma\gamma\mathrm{WW}^*$ [28], and $\mathrm{WW}^*\mathrm{WW}^*$ [29]. An additional search in the $\mathrm{b\bar{b}b\bar{b}}$ decay channel focused on the region of phase space where one $\mathrm{b\bar{b}}$ pair is highly Lorentz-boosted and is reconstructed as a single large-area jet [30]. In the cases mentioned above, at least one of the two Higgs bosons is required to decay to $\mathrm{b\bar{b}}$ to exploit the large branching fraction of this decay. Results were found to be compatible within uncertainties to the expected SM background contribution. The measurement of nonresonant HH production at the LHC with the tightest expected upper limit (15 times the SM rate) was made in the $\mathrm{b\bar{b}}\tau\tau$ channel [25], yielding an observed upper limit equivalent to 13 times the SM rate.

This article reports the results of a search for HH production with both Higgs bosons decaying into bottom quark pairs, resulting in four resolved hadronic jets. The search is performed using 13 TeV pp collisions data corresponding to an integrated luminosity of $35.9\,\mathrm{fb}^{-1}$, collected by the CMS detector in 2016. The final state containing four b quarks has the highest branching fraction of all possible HH final states, corresponding to $\approx$0.339 for an SM Higgs boson with a mass of 125 GeV. It is one of the most sensitive signatures for the investigation of HH production, as confirmed by the results of a similar search recently performed by the ATLAS Collaboration [19]. The main challenge for this analysis is the large background from multijet final states produced by quantum chromodynamics (QCD) processes, which collectively yield rates exceeding that of the signal by several orders of magnitude. We address this by fully exploiting the distinctive features of the signal: the presence of four b quarks and the kinematical properties of the decay process. In a sample selected by requiring four b quark jets, a multivariate event classifier is trained to discriminate signal from background. This sample is studied by comparing it to a model of all contributing background processes, which is completely based on data. Because of the use of different data sets, triggers, and offline selection requirements, this analysis is fully independent from the CMS searches mentioned above [18, 23, 26, 30].

JHEP04(2019)112

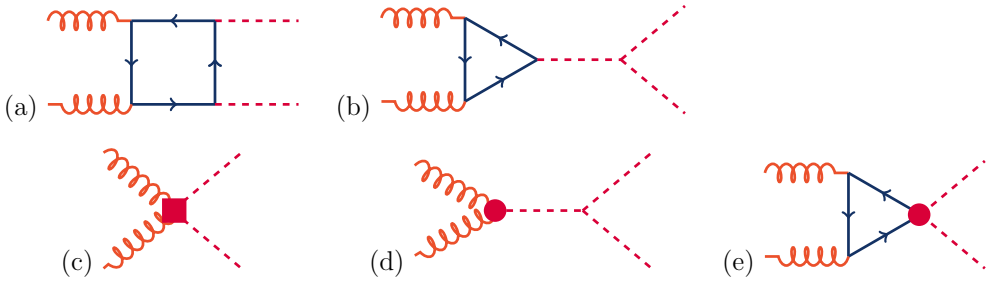

Figure 1. Feynman diagrams that contribute to HH production via gluon-gluon fusion at LO. Diagrams (a) and (b) correspond to SM-like processes, while diagrams (c), (d), and (e) correspond to pure BSM effects: (c) and (d) describe contact interactions between the Higgs boson and gluons, and (e) describes the contact interaction of two Higgs bosons with top quarks.

2 Beyond-the-standard-model extensions

In the SM, HH production occurs predominantly by gluon-gluon fusion (ggF) via an internal fermion loop, where the top quark (t) contribution is dominant. In the absence of new light states, the ggF HH production at the LHC can be generally described (considering operators up to dimension 6) by five parameters controlling the tree-level interactions of the Higgs boson. Without considering CP violating effects, the relevant part of the Lagrangian then takes the form:

$$\begin{aligned}\mathcal{L}_{\mathrm{H}} = &\frac{1}{2}\partial_\mu \mathrm{H}\,\partial^\mu \mathrm{H} - \frac{1}{2}{m_{\mathrm{H}}}^2\mathrm{H}^2 - \kappa_\lambda\,\lambda_{\mathrm{SM}} v\,\mathrm{H}^3 - \frac{m_{\mathrm{t}}}{v}\left(v + \kappa_{\mathrm{t}}\,\mathrm{H} + \frac{c_2}{v}\mathrm{HH}\right)\left(\bar{\mathrm{t}}_{\mathrm{L}}\mathrm{t}_{\mathrm{R}} + \mathrm{h.c.}\right) \\ &+ \frac{1}{4}\frac{\alpha_S}{3\pi v}\left(c_{\mathrm{g}}\,\mathrm{H} - \frac{c_{2\mathrm{g}}}{2v}\,\mathrm{HH}\right) G^{\mu\nu}G_{\mu\nu}\,.\end{aligned} \tag{2.1}$$

This Lagrangian follows from extending the SM with operators of mass dimension between four and six in the framework of an effective field theory [31], encoding the effects of new heavy states currently beyond experimental reach. The five parameters of the Lagrangian, named κ_λ, κ_{t}, c_{g}, $c_{2\mathrm{g}}$, and c_2, are related to the Higgs boson couplings. In particular, the multiplicative factors $\kappa_\lambda = \lambda_{\mathrm{HHH}}/\lambda_{\mathrm{SM}}$ and $\kappa_{\mathrm{t}} = y_{\mathrm{t}}/y_{\mathrm{SM}}$ parametrize deviations from the SM values of, respectively, the Higgs boson trilinear coupling and the top quark Yukawa coupling. The former is given by $\lambda_{\mathrm{SM}} = m_{\mathrm{H}}^2/2v^2$, with v being the vacuum expectation value of the Higgs field. The absolute couplings c_{g}, $c_{2\mathrm{g}}$, and c_2 parametrize contact interactions not predicted by the SM, i.e. the coupling of the Higgs boson to gluons and those of the two Higgs bosons to two gluons or to a top quark-antiquark pair, which could arise through the mediation of very heavy new states. In eq. (2.1), m_{t} is the mass of the top quark, and $\mathrm{G}^{\mu\nu}$ the gluon field. We neglect possible modifications of the bottom quark Yukawa coupling κ_{b}, which is already constrained by LHC data [32]. The Feynman diagrams contributing to HH production in pp collisions at leading order (LO) are shown in figure 1. The translation of the above parametrization to the flavour-diagonal Higgs basis (as discussed in ref. [31]) is trivial; we use the notation of eq. (2.1) for simplicity.

The parameter space for the Higgs boson couplings in a BSM scenario has five dimensions. Constraints on the ranges of the five parameters come from measurements of

JHEP04(2019)112

Benchmark point	κ_λ	κ_t	c_2	c_g	c_{2g}
1	7.5	1.0	-1.0	0.0	0.0
2	1.0	1.0	0.5	-0.8	0.6
3	1.0	1.0	-1.5	0.0	-0.8
4	-3.5	1.5	-3.0	0.0	0.0
5	1.0	1.0	0.0	0.8	-1.0
6	2.4	1.0	0.0	0.2	-0.2
7	5.0	1.0	0.0	0.2	-0.2
8	15.0	1.0	0.0	-1.0	1.0
9	1.0	1.0	1.0	-0.6	0.6
10	10.0	1.5	-1.0	0.0	0.0
11	2.4	1.0	0.0	1.0	-1.0
12	15.0	1.0	1.0	0.0	0.0
Box	0.0	1.0	0.0	0.0	0.0
SM	1.0	1.0	0.0	0.0	0.0

Table 1. The values of the anomalous coupling parameters for the 13 benchmark models studied [33]. For reference, the values of the parameters in the SM are also included.

single Higgs boson production already performed at the LHC, as well as other theoretical considerations [33]. However, the allowed phase space is still large and a precise scan is not feasible. The kinematical properties of the pair-produced Higgs bosons depend strongly on the values of those five couplings. A statistical approach has been developed in order to identify regions of the parameter space that have similar final state kinematical properties. The approach uses the generator-level distributions of the invariant mass of the HH system ($m_{\mathrm{HH}}^{\mathrm{gen}}$) and the modulus of the cosine of the polar angle of one Higgs boson with respect to the beam axis ($|\cos\theta^*_{\mathrm{gen}}|$) to cluster the points in the parameter space. In each region found, a representative benchmark model is selected as the point having most similar kinematical properties to the other points in the region. The procedure, described in ref. [33], leads to twelve benchmarks that taken together best represent, within a limited uncertainty, the phenomenology of the whole five-dimensional space. An additional benchmark (box), representative of the null Higgs boson self-coupling hypothesis, is also considered. The parameter values of the benchmarks are listed in table 1. The search for BSM signals presented here is focused on these benchmarks.

3 The CMS detector

The CMS detector is a multipurpose apparatus designed to reconstruct the high-energy interactions produced by the LHC. Its central feature is a superconducting solenoid with an internal diameter of 6 m. The solenoid generates a magnetic field of 3.8 T inside a volume occupied by four main sub-detectors, each composed of a barrel and two endcap sections: silicon pixel and strip tracker detectors, a lead tungstate crystal electromagnetic calorimeter (ECAL), and a brass and scintillator hadron calorimeter (HCAL). The pixel

JHEP04(2019)112

tracker provides an impact parameter resolution for charged tracks of about 15 μm, which allows for a precise reconstruction of secondary vertices, crucially used to identify jets originating from the hadronization of b quarks (b jets). Muons are measured in gas-ionization detectors embedded in a steel flux return yoke outside the solenoid. Information from the calorimeters and muon detectors is used by the first level of the CMS trigger [34], a system based on custom hardware processors that provides the first online event selection. The second level of the CMS trigger, also called high-level trigger and consisting of a farm of processors running a version of the full event reconstruction software optimized for fast processing, further selects events using information from the whole detector before sending them downstream for detailed processing and storage. Particles produced in the pp collisions are detected in the pseudorapidity range $|\eta| < 5$. Pseudorapidity is defined as $|\eta| = -\ln\tan(\theta/2)$, where the polar angle θ is measured from the z-axis, which points along the beam direction toward the Jura mountains from LHC Point 5. A more detailed description of the CMS detector can be found in [35].

4 Data sets

The online event selection for the data used in this analysis is designed to select a sample of multijet events enriched with b quark decays, reducing the rate from the QCD multijet background with light quarks and gluons. The combined secondary vertex (CSVv2) algorithm [36] is used to identify b jets. This algorithm exploits the relatively long lifetime of hadrons containing b quarks ($c\tau \sim 450\,\mu$m), which results in a displaced decay point of the produced b hadrons. The reconstructed trajectories of charged decay products from b hadrons thus exhibit significant impact parameters with respect to the b quark production point. The CSVv2 algorithm uses the impact parameter information together with information on other characteristics of the jets to discriminate jets originating from b quarks from those produced by the hadronization of light quarks or gluons. Two trigger paths contribute to the online selection. In the first trigger path jets are considered if their momentum transverse to the beam direction, p_{T}, is above 30 GeV and $|\eta| < 2.6$. Selected events must contain at least four such jets of which at least three are tagged as b jets by the CSVv2 algorithm and at least two have $p_{\mathrm{T}} > 90$ GeV. The second trigger path requires at least four jets with $p_{\mathrm{T}} > 45$ GeV with at least three tagged as b jets by the CSVv2 algorithm. The logical OR between these two selections provides the data used in this analysis.

The production of nonresonant HH in the SM is simulated following the prescriptions of ref. [37] at LO with MadGraph5_aMC@NLO 2.2.2 [38] used as the generator. Loop factors are calculated on an event-by-event basis and applied to an effective model, from ref. [37]; the NNPDF30_lo_as_0130_nf_4 PDF set [39] is used. In addition, for the study of BSM models involving anomalous Higgs boson couplings, we generate for each of the parameter space points listed in table 1 a set of 300 000 simulated events.

The 14 simulated signal samples are added together to obtain a larger signal sample. We will refer to this ensemble of events as the Pangea sample. This sample is then reweighted to reproduce the physics of any particular point in the BSM phase space. The

JHEP04(2019)112

weights are obtained by looking at the matrix element information for $m_{\mathrm{HH}}^{\mathrm{gen}}$ and $\cos\theta_{\mathrm{gen}}^{*}$ from dedicated simulations, as described in ref. [40]. The numbers of events used to determine the weights at generator level are 3 000 000 for the SM sample and 50 000 for each BSM benchmark. In the following, we always use the Pangea sample instead of the 14 original samples to study signal properties in each model considered.

Although our search employs an approach fully based on data to model backgrounds, we make use of a simulation of QCD processes for several cross-checks. This simulation consists of a collection of seven simulated data sets of contiguous ranges in the $H_{\mathrm{T}}^{\mathrm{gen}}$ variable, which is defined as the scalar sum of the p_{T} of all partons that originate from the hard-scattering process in a simulated event. The samples are generated by MadGraph5_aMC@NLO 2.2.2 at LO, using the NNPDF30_lo_as_0130 set, and are then interfaced with pythia 8.212 [41] for fragmentation and parton showering, using the MLM matching [42]; their equivalent integrated luminosity depends on the $H_{\mathrm{T}}^{\mathrm{gen}}$ range considered and increases from 0.06 to 400 fb^{-1} as $H_{\mathrm{T}}^{\mathrm{gen}}$ varies between 200 and 2000 GeV. For additional studies of the sub-dominant background from top quark pairs, a large next-to-leading order (NLO) powheg 2.0 [43–45] sample of inclusive $\mathrm{t\bar{t}}$ [46] events is used. The behaviour of minor backgrounds is verified and a study of their contamination of our selected sample is carried out using powheg 2.0 NLO samples of single top quark t channel [47], $\mathrm{t\bar{t}H}$ [48], single Higgs boson production [49], and associated ZH production [50]. In addition, we use single top quark s channel, $\mathrm{t\bar{t}t\bar{t}}$, $\mathrm{t\bar{t}b\bar{b}}$, and $\mathrm{b\bar{b}H}$ samples generated with MadGraph5_aMC@NLO 2.2.2 at NLO. All of those samples are interfaced with pythia 8.212 for parton showering and fragmentation. The $\mathrm{t\bar{t}}$ sample utilises the generator tune CUETP8M2T4 [51] for the underlying event activity, other samples interfaced with pythia use the tune CUETP8M1 [52]. The $\mathrm{t\bar{t}}$, $\mathrm{t\bar{t}H}$, single Higgs boson, and ZH samples are generated using the NNPDF30_nlo_as_0118 PDF set. The single top quark, $\mathrm{t\bar{t}b\bar{b}}$, and $\mathrm{b\bar{b}H}$ samples are generated with the NNPDF30_nlo_nf_4_pdfas set. The NNPDF30_nlo_nf_5_pdfas set is used to generate the $\mathrm{t\bar{t}t\bar{t}}$ sample. All of the PDF sets are taken from the LHAPDF6 set [53]. The response of the CMS detector is modelled using Geant4 [54].

Finally, in order to study possible discrepancies between the efficiency of the triggers used in our data selection and their modelling by the simulation, we compare the effect of b jet selection requirements on data collected by a trigger requiring a single isolated muon of $p_{\mathrm{T}} > 18$ GeV with its simulation, using a mixture of events from $\mathrm{t\bar{t}}$/single-top described above and a MadGraph5_aMC@NLO 2.2.2 W+jets LO sample using the MLM matching, weighted appropriately, and a W+jets sample generated using the NNPDF30_lo_as_0130 PDF set.

5 Event reconstruction

Global event reconstruction is performed by the particle-flow (PF) algorithm [55], which aims to reconstruct and identify each individual particle in an event, with an optimized combination of information from the various elements of the CMS detector. In this process, the identification of the particle type (photon, electron, muon, charged hadron, neutral

JHEP04(2019)112

hadron) plays an important role in the determination of the particle direction and energy. Electrons (e.g. coming from photon conversions in the tracker material or from b hadron semileptonic decays) are identified as a primary charged particle track and one or more ECAL energy clusters corresponding to this track extrapolation to the ECAL and to possible bremsstrahlung photons emitted along the way through the tracker material. Muons (e.g. from b hadron semileptonic decays) are identified as a track in the central tracker consistent with either a track or several hits in the muon system, associated with an energy deficit in the calorimeters. The objects primarily considered in this analysis are hadronic jets, composed of particles produced by quark fragmentation and hadronization. The energy of charged hadrons is determined from a combination of their momentum measured in the tracker and the matching ECAL and HCAL energy deposits, corrected for zero-suppression effects and for the response function of the calorimeters to hadronic showers. The energy of neutral hadrons is obtained from the corresponding corrected ECAL and HCAL energy. Jets are reconstructed from PF candidates using the anti-k_{T} clustering algorithm [56] with a distance parameter of 0.4, as implemented in the FastJet package [57]. Jet energy corrections are applied to both data and simulation to scale the energy and correct for differences in the detector response in real and simulated collisions [58]. Jet identification criteria are also applied in order to reject fake jets from detector noise and jets originating from primary vertices not associated with the hard interaction [59]. The combined multivariate algorithm (cMVAv2) [36] is used in the offline analysis to identify jets that originate from the hadronization of b quarks. The cMVAv2 builds on the CSV algorithm by adding soft-lepton information to the combined discriminant. The value of the multivariate discriminant used depends on the required suppression of jets from light quarks and gluons. The medium working point of the cMVAv2, defined such that the misidentification rate of light quarks and gluons as b jets is 1%, is used in this analysis. For jets produced by the hadronization of b quarks emitted in HH production events, the medium working point corresponds to a b-tagging efficiency of about 65% for the jets of interest of this analysis.

A weight is applied to each Monte Carlo (MC) event in order to match the distribution of the number of primary interactions per event in data (pileup correction), thus reproducing the effect on the selection efficiency of the varying instantaneous luminosity conditions incurred during data taking. The simulated events are also weighted to account for measured differences in the b tagging efficiency between data and simulation [36]. The trigger efficiency for signal events is evaluated using a full simulation of the trigger [34]. The correction factor for the efficiency is found to be 0.96 ± 0.02 based on measurements performed in b-tag multiplicity categories, using a top-pair enriched sample collected with an inclusive muon trigger.

6 Analysis strategy

The focus of this search is the study of nonresonant production of HH in the $\mathrm{b\bar{b}b\bar{b}}$ final state, as predicted by the SM and by several BSM extensions. The analysis is optimized for sensitivity to the SM signal. We use the same selection to extract limits on the HH production cross section for the BSM models.

JHEP04(2019)112

The offline selection, performed on all data events passing one of the two trigger paths described in section 4, aims at increasing the fraction of data events containing two Higgs boson candidates decaying into b quark jet pairs. This includes a preliminary selection of events where four or more jets have been b-tagged by the cMVAv2. Although this selection significantly reduces the QCD multijet background rate, this background still dominates the selected data, with contributions from events where light quark or gluon jets are mistagged by the cMVAv2 and events containing heavy quarks.

After the selection of events with four or more b tags, each reconstructed Higgs boson candidate is composed of a pair of b jets, referred to in the following as "a dijet system" or simply "dijet". A boosted decision tree (BDT) classifier [60] is then trained to exploit the observable differences between the SM signal and the background. Finally, a search for a signal contribution to the selected data and an extraction of an upper limit in the number of selected signal events is performed by means of a binned fit to the distribution of the BDT classifier output. The limit on the number of events is converted to a limit on the HH production cross section times the square of the branching fraction of the Higgs boson into a $\mathrm{b\bar{b}}$ pair, using the corresponding integrated luminosity and the computed signal efficiency.

Both the optimization of the BDT classifier and the extraction of upper limits on HH production require an accurate modelling of the multijet background. Unfortunately, the precise simulation of QCD processes yielding a large number of final-state partons is notoriously hard, as MC simulations are not complete to beyond LO; in addition, the very large production cross section for those processes makes it wholly impractical to produce simulated data sets corresponding to an integrated luminosity comparable to that of collision data. To address these issues, a dedicated method, fully based on data, was developed to produce a precise model of the kinematical behaviour of background events. This is described in detail in section 8.

7 Event selection

The events of interest are identified by a jet-based selection applied to data collected by the triggers described in section 4, as well as to all simulated samples. Jets are required to have $p_{\mathrm{T j}} > 30\,\mathrm{GeV}$ and $|\eta_{\mathrm{j}}| < 2.4$. We require at least four such jets ($N_{\mathrm{j}} \geq 4$) and these need to be defined as b-tagged jets by the medium working point of the cMVAv2 ($N_{\mathrm{b}} \geq 4$). These criteria strongly reduce the QCD multijet background and select HH production events where the final state can be fully reconstructed. The number of selected events in the data set studied is 184 879.

The efficiencies for the SM signal are listed in table 2. The efficiency for the 13 BSM points varies from -40% to +10% compared to the SM values. The average number of jets per selected event is ≈5. The four jets with the highest cMVAv2 discriminant values are considered as the decay products of two Higgs boson candidates. The pairing of the four jets into Higgs boson candidates is performed by considering the invariant mass of the two dijet candidates calculable for the three possible pairings, and computing the absolute mass differences $\Delta \mathrm{M}_{klmn} = |\mathrm{M}_{kl} - \mathrm{M}_{mn}|$, where the $klmn$ indices run on the three permutations of the four jets. The combination resulting in the smallest mass difference

JHEP04(2019)112

	Produced	Trigger	≥4 b tags
N events / fb	11.4	3.9	0.22
Relative eff.		34%	5.6%
Efficiency		34%	1.9%

Table 2. Cut-flow efficiency for the SM signal pp → HH → $b\bar{b}b\bar{b}$; the efficiency and the relative reduction of each successive selection step is shown. The number of expected SM signal events for an integrated luminosity of $1\,\text{fb}^{-1}$ is also reported.

between the two dijet systems is chosen as the one best describing the decay topology. This procedure results in a correct pairing of the b quarks to Higgs bosons in 54% of the cases, as tested on the Pangea MC signal sample. The two selected dijets are then labelled as "leading" and "trailing" according to their invariant mass value. This procedure, which does not explicitly use the known mass of the Higgs boson, allows the dijet masses for the selected combinations to retain the power to discriminate the HH production signal from the background.

A multivariate technique is used in order to improve the sensitivity of the analysis. A BDT discriminator is trained to distinguish the SM signal from backgrounds (as described in section 8), using the XGBoost library [60]. All 13 BSM models use the same BDT as the SM to distinguish signal from background. We supply the BDT algorithm with a set of variables describing the kinematical properties of the event. The list of variables is pruned to discard those not contributing to the overall discrimination power of the algorithm. In table 3 we list the variables chosen to build the classifier. In order to characterise the HH system we use as mass variables the invariant mass of the HH system (M_{HH}), an estimator of the combined mass of the HH system, M_{X} (defined by eq. (7.1) below), and the invariant masses of the reconstructed Higgs boson candidates (M_{H_1}, M_{H_2}). The p_{T} of the HH system and of each Higgs boson candidate ($p_{\text{T}}^{\text{H}_1\text{H}_2}$, $p_{\text{T}}^{\text{H}_1}$ and $p_{\text{T}}^{\text{H}_2}$) are used as well as the $\Delta R = \sqrt{(\Delta\eta)^2 + (\Delta\phi)^2}$ and $\Delta\phi$ angles between the jets that form each reconstructed Higgs boson ($\Delta R_{\text{jj}}^{\text{H}_1}$, $\Delta R_{\text{jj}}^{\text{H}_2}$, $\Delta\phi_{\text{jj}}^{\text{H}_1}$ and $\Delta\phi_{\text{jj}}^{\text{H}_2}$). Additionally, we use the θ^* angles between the HH system and the leading Higgs boson candidate, $\cos\theta^*_{\text{H}_1\text{H}_2-\text{H}_1}$, and between the leading Higgs boson candidate and the leading jet, $\cos\theta^*_{\text{H}_1-\text{j}_1}$. We further use the following jet-related variables: the $p_{\text{T}}^{\text{j}_i}$ and η_{j}^i ($i = 1$–4) of the four jets with the highest values of the cMVAv2 discriminant, the scalar p_{T} sum of the jets in the event (H_{T}), and of the jets that are not part of the reconstructed HH system (i.e. the rest of the jets, $H_{\text{T}}^{\text{rest}}$). The cMVAv2 values of the third and fourth jets sorted by cMVAv2 value ($CMVA_3$ and $CMVA_4$) are also used. The estimator, M_{X}, of the mass of the system of two Higgs bosons is constructed as:

$$M_{\text{X}} = m_{4\text{j}} - \Big(M_{\text{H}_1} - m_{\text{H}}\Big) - \Big(M_{\text{H}_2} - m_{\text{H}}\Big), \tag{7.1}$$

where $m_{\text{H}} = 125\,\text{GeV}$. Even though M_{X} is strongly correlated with other variables used in the BDT, its use improves the discrimination power.

The invariant masses of the reconstructed Higgs boson candidates are the variables with the largest discrimination power, but all the variables used make significant contributions to the classifier.

JHEP04(2019)112

HH system	H candidates	Jet variables
M_{X}, M_{HH},	M_{H_1}, M_{H_2}	$p_{\mathrm{T}}^{\mathrm{j}\,(i=1\text{–}4)}$, $\eta_{\mathrm{j}}^{(i=1\text{–}4)}$,
$p_{\mathrm{T}}^{\mathrm{H}_1\mathrm{H}_2}$	$p_{\mathrm{T}}^{\mathrm{H}_1}$, $p_{\mathrm{T}}^{\mathrm{H}_2}$	$H_{\mathrm{T}}^{\mathrm{rest}}$, H_{T}
$\cos\theta^*_{\mathrm{H}_1\mathrm{H}_2-\mathrm{H}_1}$	$\cos\theta^*_{\mathrm{H}_1-\mathrm{j}_1}$	$CMVA_3$, $CMVA_4$
	$\Delta R_{\mathrm{jj}}^{\mathrm{H}_1}$, $\Delta R_{\mathrm{jj}}^{\mathrm{H}_2}$, $\Delta\phi_{\mathrm{jj}}^{\mathrm{H}_1}$, $\Delta\phi_{\mathrm{jj}}^{\mathrm{H}_2}$	

Table 3. List of BDT input variables.

We use 60% of the Pangea sample for training the classifier. The remaining 40% of the Pangea sample is employed for the validation (20%) and application (20%) steps; this splitting has been found to produce maximal sensitivity to a possible HH signal. As a background sample, an artificial data set constructed with a custom mixing procedure, as described in section 8, is employed.

8 The background model

A method exploiting collision data only, based on hemisphere mixing, has been developed [61] to perform two separate tasks: first, to provide input to the training of the BDT classifier; and second, to reproduce the expected shape of the BDT output in background-only events. The method does not require the presence of signal-depleted sidebands in order to extract a background estimation; in fact, it aims at creating an artificial background data set using the whole original data set as the input. Thus, rather than a model of a single distribution, a full model of the original data is produced.

8.1 The hemisphere mixing technique

The basic concept at the heart of the method is to divide each data event in two hemispheres. The collection of hemispheres can then be used to create new events by recombining them in pairs. To create a good background model, the kinematical properties of the new events must be as similar as possible to the ones of the original data but also insensitive to the possible presence of signal. In order to define the hemispheres, we use the transverse thrust axis. This is defined as the axis on which the sum of the absolute values of the projections of the p_{T} of the jets is maximal, and correspondingly, transverse thrust (T) is the value of this sum. Once the transverse thrust axis is identified, the event is divided into two halves by cutting perpendicular to the transverse thrust axis. One such half is called a hemisphere (h). In a preliminary step, each event in the original N-event data set is split into two hemispheres that are collected in a library of $2N$ elements. Once the library is created, each event is used as a basis for creating artificial events. These are constructed by picking two hemispheres from the library that are *similar*, according to a measure defined below, to the two hemispheres that make up the original event. An illustration of the procedure can be found in figure 2.

The number of jets N_{j}^h and number of b-tagged jets N_{b}^h in each hemisphere, together with four jet-related variables, are used to define a hemisphere similarity criterion. The

JHEP04(2019)112

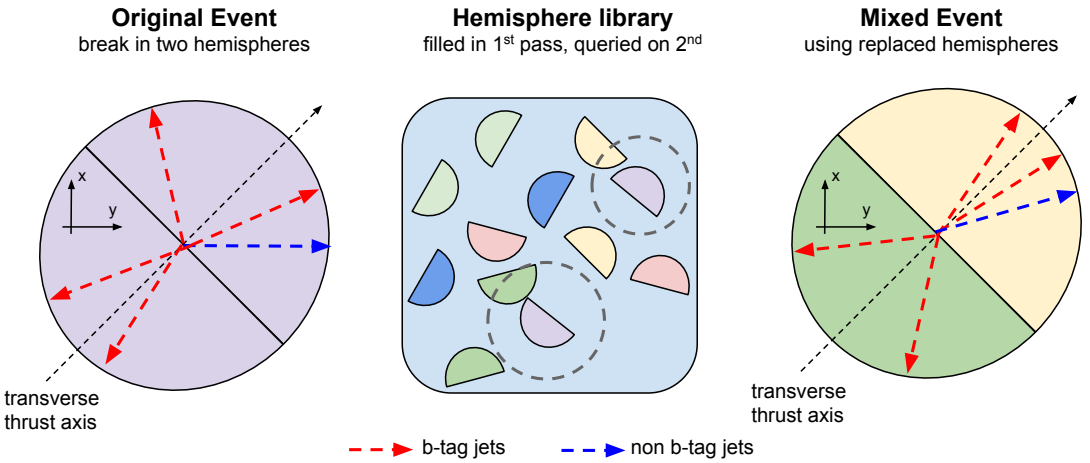

Figure 2. An illustration of the hemisphere mixing procedure. The transverse thrust axis is defined as the axis on which the sum of the absolute values of the projections of the p_{T} of the jets is maximal. Once the thrust axis is identified, the event is divided into two halves by cutting along the axis perpendicular to the transverse thrust axis. One such half is called a hemisphere (h). In a preliminary step, each event in the original N-event data set is split into two hemispheres that are collected in a library of $2N$ hemispheres. Once the library is created, each event is used as a basis for creating artificial events. These are constructed by picking two hemispheres from the library that are similar to the two hemispheres that make up the original event.

four variables are the combined invariant mass of all jets contained in the hemisphere M^h_{tot}, transverse thrust of the hemisphere T^h, the scalar sum of the projections of the p_{T} of all the jets onto the axis orthogonal to the thrust axis on the transverse plane, T^h_a, the projection of the vectorial sum of the momenta of the jets along the beam axis, Σp^h_z. If we label the original hemisphere o, and q the one in the library that is compared to o, the number of jets in o and q is required to be equal, $N^o_{\mathrm{j}} = N^q_{\mathrm{j}}$, and also the number of b-tagged jets are required to be equal, $N^o_{\mathrm{b}} = N^q_{\mathrm{b}}$. These two requirements are used to maintain the topology of the original events and to avoid introducing events that would not pass the selection described in section 7 (e.g. by combining a hemisphere with 2 jets with a hemisphere with 1 jet, resulting in an event with 3 jets). The requirement for equal numbers of jets is waived for the infrequently occurring pairs of hemispheres that both have at least four jets and at least four b-tagged jets. For each hemisphere q in the library fulfilling the above criteria, a multidimensional distance from hemisphere o is computed using the four jet-related variables, as follows:

$$D(o,q)^2 = \frac{(M^o_{\mathrm{tot}} - M^q_{\mathrm{tot}})^2}{V(M_{\mathrm{tot}})} + \frac{(T^o - T^q)^2}{V(T)} + \frac{(T^o_a - T^q_a)^2}{V(T_a)} + \frac{(|\Sigma p^o_z| - |\Sigma p^q_z|)^2}{V(\Sigma p_z)}. \tag{8.1}$$

In the equation above, $V(x)$ represents the variance for the variable x, within the subset of events of given N_{b} and N_{j} characterizing the hemisphere in question. Once all $D(o,q)$ are computed, the kth nearest-neighbour hemisphere in the library, with $k \geq 1$ (i.e. the one such that $0 = D(o,0) < \ldots < D(q,k)$) can be chosen to model the corresponding hemisphere of the original event; the nearest hemisphere, corresponding to $k = 0$, is by construction

JHEP04(2019)112

the original one. We match the Σp_z variables by considering only their absolute value (assuming forward-backward symmetric detector acceptance to jets, as is safe to do in the case of the CMS detector) and invert the sign of jet Σp_z components in one of the two matched hemispheres (q_1 and q_2) if $\mathrm{sgn}(\Sigma p_z^{o_1} \Sigma p_z^{o_2}) \neq \mathrm{sgn}(\Sigma p_z^{q_1} \Sigma p_z^{q_2})$, where indices o_1 and o_2 are the two hemispheres of the original event. Finally, the four-vectors of the jets contained in the two hemispheres are rotated along the ϕ coordinate to match the original transverse thrust axis of the modelled event. To keep track of the distance criterion used to choose each hemisphere, the artificial event may be labelled as (k_1, k_2) using the neighbour indices, indicating that one hemisphere of the original event was replaced by its k_1th neighbour and the other hemisphere of the original event by its k_2th neighbour and these were used to form the artificial event. By applying this procedure to the whole set of events of the data to be modelled, and by choosing a limiting value K for k, we obtain a total of K^2 data sets, each equal in size to the original one, and each featuring very similar characteristics to the original one, despite being made up entirely of artificial events.

The procedure described above is successful at modelling multijet events because it exploits the fact that their production can be idealized at LO as a $2 \to 2$ process, which is made complex by a number of sub-leading effects (QCD radiation, pileup, multiple interactions). The reconstruction of the transverse thrust axis, and the decomposition of events into hemispheres using that axis as a seed, uses the independent fragmentation of the two final state partons as a working hypothesis to create artificial replicas of the original events. The method destroys any correlation in the jet distribution between the two hemispheres, so that any physical effect, such as the decay of a heavy object into jet pairs, is washed out in the artificial samples. Because of this, the resulting artificial data sets are unaffected by the presence of a small signal contamination in the original data. This has been verified by signal injection tests. We started with an original data set composed of simulated QCD multijet events to which is added an additional component of signal corresponding to a cross section 100 times larger than the one expected by the SM. After hemisphere mixing, the kinematical properties of the resulting artificial samples are found to resemble closely those from the QCD multijet part of the original data set, which is its dominant component, and unaffected by the minority component (the signal contamination). Naively this can be understood if we note that, if the signal fraction in the original sample amounts to e.g. 0.1%, the probability that a signal event is modelled using two different hemispheres both originally belonging to signal events is of the order of 0.0001%. Event-based variables such as the two Higgs boson candidate masses, which are obtained by the minimum ΔM criterion described in section 7 and are thus sensitive to the characteristics of both hemispheres together, do not retain their distribution in events where only one hemisphere is taken from an HH decay event.

We apply the hemisphere mixing technique to data events selected with the $N_\mathrm{j} \geq 4$, $N_\mathrm{b} \geq 4$ criteria, using $K = 10$ neighbour hemispheres to each hemisphere of the original event, which were found to still provide good modelling. The resulting artificial samples are used to provide a background model in the training of the BDT classifier (training sample), as well as an independent set for the BDT validation and optimization (validation sample), and a third data set used to extract the predicted shape of the optimized BDT

JHEP04(2019)112

(application sample). Not all of the data sets are fully independent so only a subset can be safely employed for further studies. We use the following collections of artificial events in the measurement: for the training sample, we use all artificial events of types $(1,1)$, $(1,2)$, $(2,1)$, and $(2,2)$; for the validation sample, all artificial events of types $(3,4)$, $(5,6)$, $(7,8)$, and $(9,10)$; and for the application sample, all artificial events of types $(4,3)$, $(6,5)$, $(8,7)$, and $(10,9)$. This split guarantees that the three samples have equal number of events, and that the validation and application samples are independent of each other, being constituted of artificial events made up of different hemispheres. For the training sample the partial use of the same hemispheres in modelling different artificial events might at most slightly degrade the discrimination power but does not have a detrimental effect on the subsequent steps of the analysis. A study is performed by switching the validation and application samples and we find that this does not change the results. The fraction of data events that are totally replicated in the background template is completely negligible. A comparison between the distributions obtained through the procedure described above and by using MC simulation for QCD multijet processes can be seen in figure 3 for a number of variables. The compatibility is good, although the statistical uncertainties in the model from MC simulation are large.

8.2 The background template validation

We perform a number of stringent checks to verify that the background is well modelled by the hemisphere mixing procedure. For this purpose, we define two control regions (CRs): the first one, called the m_{H} CR, is obtained by removing from the data events where the leading and trailing dijet masses are in the region $90 < M_{\mathrm{H}_1} < 150\,\mathrm{GeV}$, $80 < M_{\mathrm{H}_2} < 140\,\mathrm{GeV}$. This avoids using events belonging to the signal-enriched region. In the second region, the b tag CR, fully orthogonal to the default selection, we select events with at least four b-tagged jets as defined by the loose working point of the cMVAv2, while vetoing events with any jets that are defined as b-tagged jets according to the medium working point of the cMVAv2. The loose working point of the cMVAv2 has a misidentification rate of ≈10% and a b-tagging efficiency of ≈85% for jets produced by the hadronization of b quarks emitted in HH production events. The distributions of all individual event variables for the artificial data sets are compared to those from the original data set in these two CRs and are found to be in agreement. This is illustrated for a number of variables in figures 4 and 5. However, the power of the technique rests in its ability to provide fully multidimensional modelling. To verify this, a first cross-check consists of comparing the full BDT shape for data and the artificial model in the m_{H} CR. We observe an agreement in the shape of the BDT discriminator with a slight excess of background events in the lower range of the BDT output (as can be seen in figure 6, left). A similar trend is seen in the b tag CR.

A high-precision study is required to investigate the need for a correction to the background shape of the BDT discriminator and a corresponding systematic uncertainty. For this purpose, all the possible combinations of neighbouring hemispheres in the range 1 to 10, except the ones used for training $((1,1),(1,2),(2,1),(2,2))$, are merged into a unique sample M. We re-sample 200 new replicas with the same number of events as the original

JHEP04(2019)112

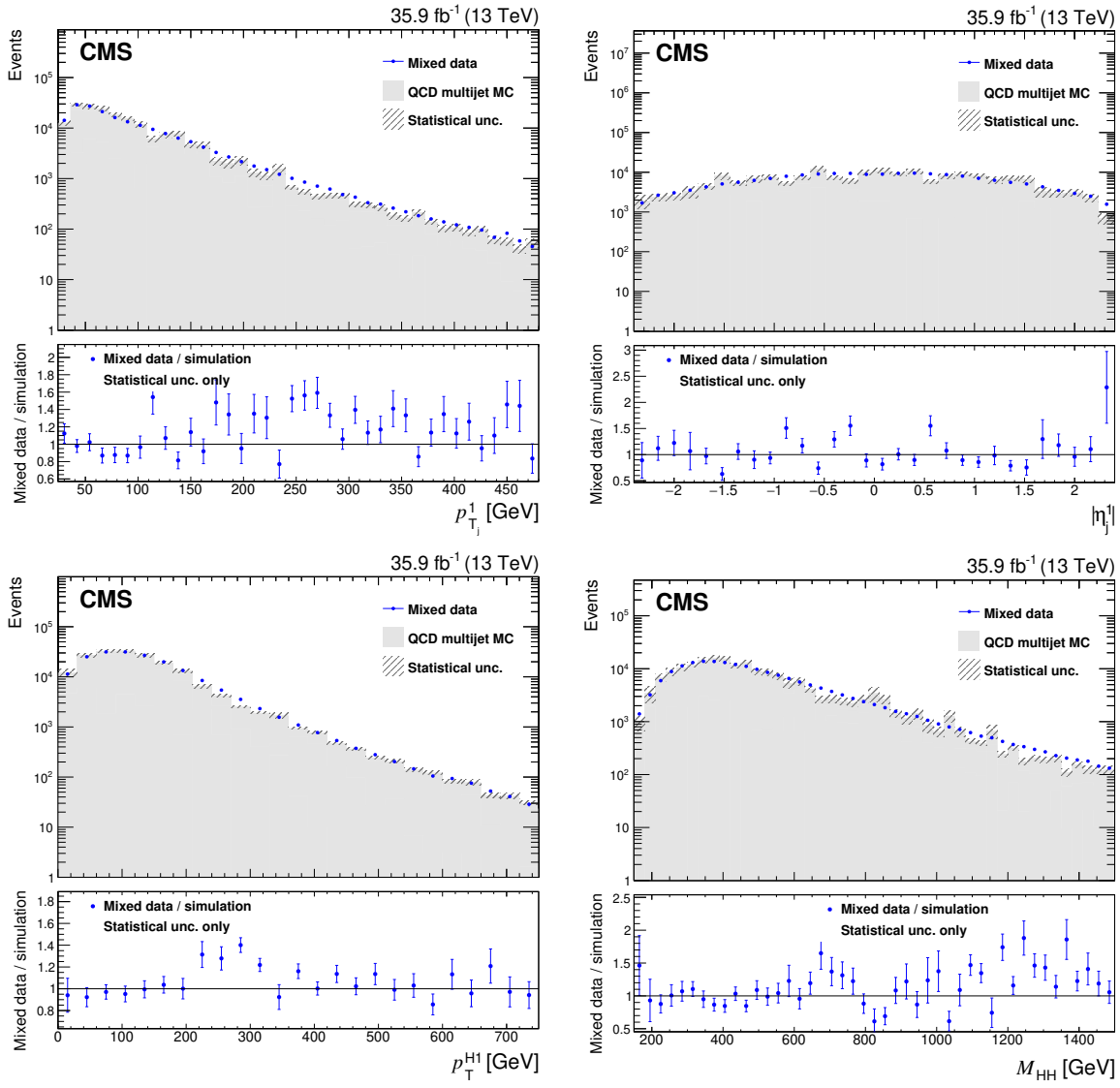

Figure 3. Comparison between the background model obtained with the hemisphere mixing technique and MC simulation of QCD multijet processes for $p_{\mathrm{T}}^{\mathrm{j}_1}$ (upper left), η_{j}^{1} (upper right), $p_{\mathrm{T}}^{\mathrm{H}_1}$ (lower left), and M_{HH} (lower right). Bias correction for the background model, described in section 8.2, is applied by rescaling the weight of each event using the event yield ratio between corrected and uncorrected BDT distributions. Only statistical uncertainties are shown as the uncertainties related to the bias correction can not be propagated from the BDT classifier to a different variable.

JHEP04(2019)112

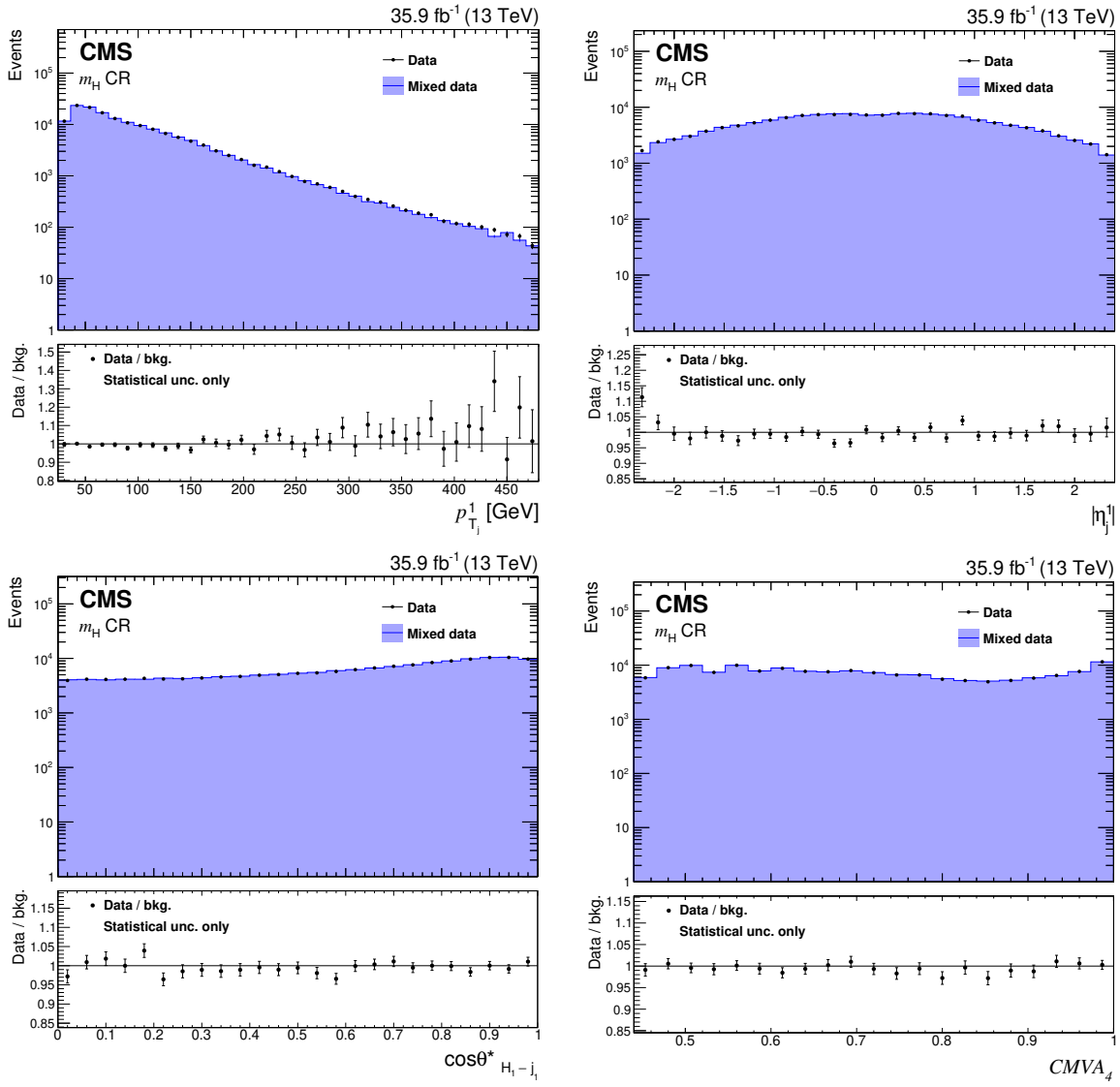

Figure 4. Comparison between the background model obtained with the hemisphere mixing technique and data in the m_{H} CR for the variables $p_{\mathrm{T}}^{\mathrm{j}_1}$ (upper left), η_{j}^{1} (upper right), $\cos\theta^{*}_{\mathrm{H}_1-\mathrm{j}_1}$ (lower left), and $CMVA_4$ (lower right). Bias correction for the background model, described in section 8.2, is applied by rescaling the weight of each event using the event yield ratio between corrected and uncorrected BDT distributions in this CR. Only statistical uncertainties are shown as the uncertainties related to the bias correction can not be propagated from the BDT classifier to a different variable.

JHEP04(2019)112

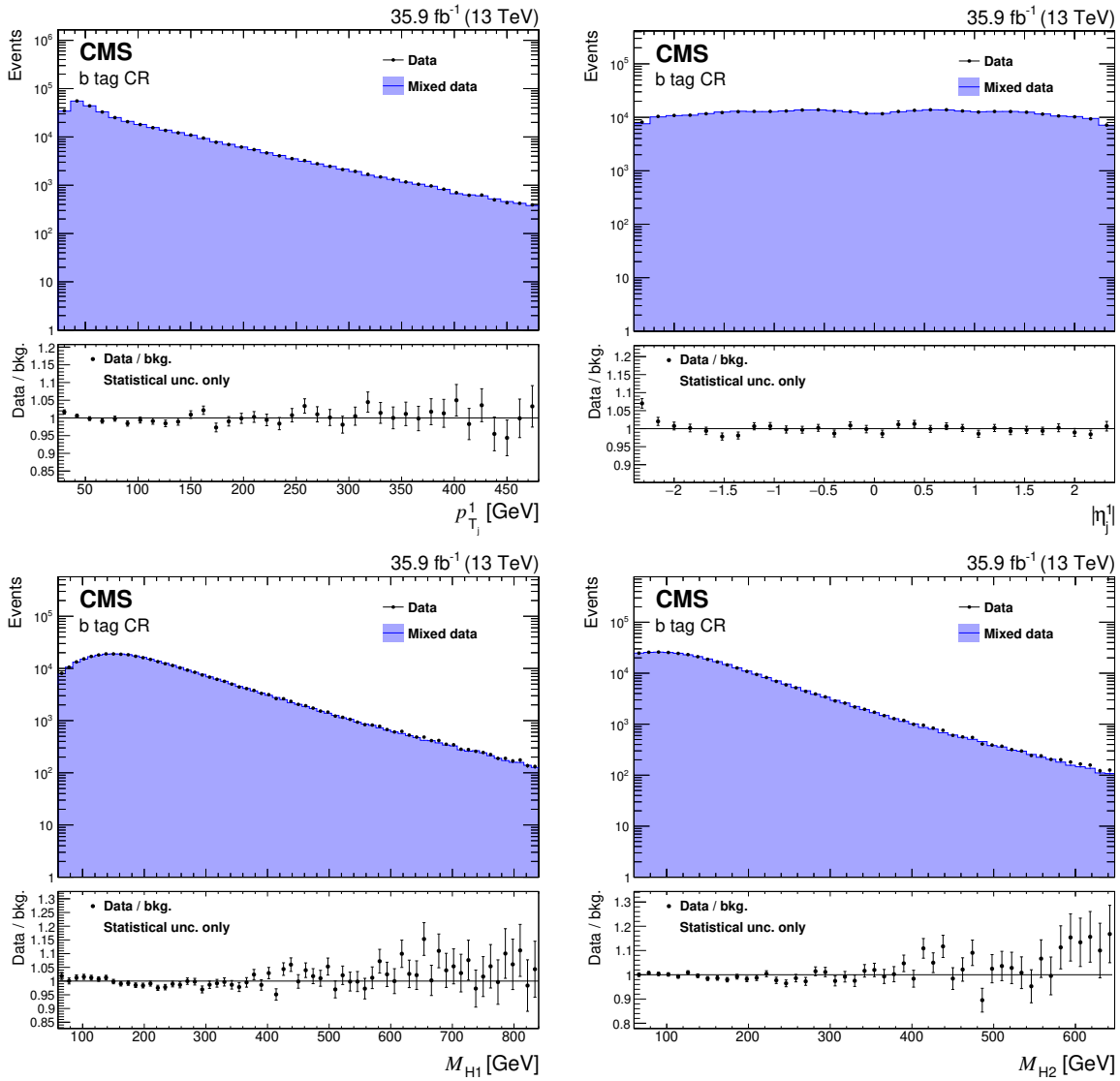

Figure 5. Comparison between the background model obtained with the hemisphere mixing technique and data in the b tag CR for the variables $p_{\mathrm{T_j}}^1$ (upper left), η_{j}^1 (upper right), $M_{\mathrm{H_1}}$ (lower left), and $M_{\mathrm{H_2}}$ (lower right). Bias correction for the background model, described in section 8.2, is applied by rescaling the weight of each event using the event yield ratio between corrected and uncorrected BDT distributions in this CR. Only statistical uncertainties are shown as the uncertainties related to the bias correction can not be propagated from the BDT classifier to a different variable.

data set without replacement from M, each time starting from the full sample M. Each of the replicas is then used as a new original data set, and artificial samples are created from it using the hemisphere mixing procedure. The output distribution of a previously trained BDT for the large sample M is then compared to that for its artificial counterpart, obtaining a distribution of differences between actual and predicted data in each of the 80 BDT bins. A schematic of the procedure and the results are available in appendix A. A systematic bias is detected and the background template is corrected for the value obtained from

JHEP04(2019)112

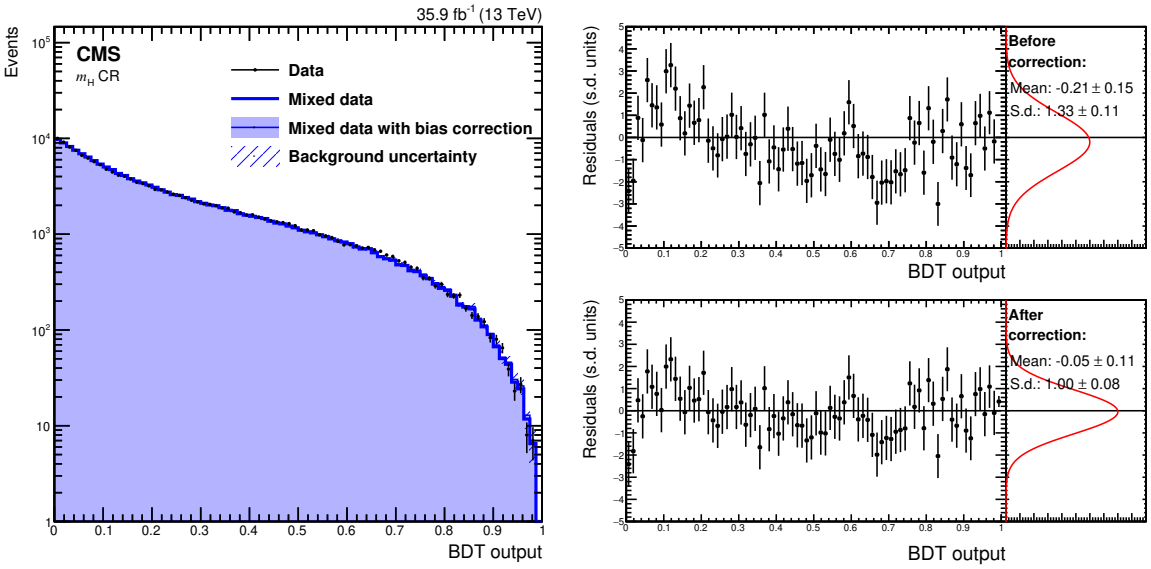

Figure 6. Left: comparison of the distribution of BDT output for data (left) selected in a region of the leading versus trailing Higgs boson candidate mass plane that excludes a 60- GeV-wide box around the most probable values of the dijet masses of signal events, with the corresponding output on an artificial sample obtained from the same data set by hemisphere mixing. Right: bin-by-bin differences between data and model, in s.d. units before (upper right) and after (lower right) bias correction; pull distribution for the differences, fit to a Gaussian distribution. The bias correction uncertainty is increased to take the s.d. of the residuals to 1.0.

this comparison. The variance related to the background bias extraction, together with expected statistical uncertainty, are estimated and accounted for as a systematic uncertainty in the final fit described in section 10. The validity of this background bias extraction procedure has been checked by applying it to the data in the two CRs previously mentioned. The means of the per bin expectation values minus the observed values are compatible with zero after the bias correction in both control regions, the root-mean-square of the pulls is compatible with one after the bias correction in the b tag CR, but not in the m_{H} CR, as shown on figure 6 (upper right). To account for this, we increase the uncertainty in the background such that the value of standard deviation (s.d.) becomes 1.0 in the m_{H} CR after the bias correction is applied (figure 6, lower right).

9 Systematic uncertainties

The sources of systematic uncertainties found to be relevant to this analysis are listed in table 4. The systematic uncertainty in the shape of the background model is accounted for by assigning an uncertainty to each BDT output bin that includes the statistical uncertainty and the systematic uncertainty related to the bias extraction discussed in the previous section. The background normalization is left freely floating in the BDT distribution fit. The uncertainty due to the b tagging efficiencies is estimated by varying them within their uncertainties. The uncertainty due to the pileup modelling is computed by considering

JHEP04(2019)112

Source	Affects	Exp. limit variation
Bkg. shape	bkg.	30%
Bkg. norm.	bkg.	8.6%
b tagging eff.	sig	2.8%
Pileup	sig	<0.01%
Jet energy res.	sig	<0.01%
Jet energy scale	sig	<0.01%
Int. luminosity	sig	<0.01%
Trigger eff.	sig	<0.01%
μ_F and μ_R scales	sig	<0.01%
PDF	sig	<0.01%

Table 4. Systematic uncertainties considered in the analysis and relative impact on the expected limit for the SM HH production. The relative impact is obtained by fixing the nuisance parameters corresponding to each source and recalculating the expected limit.

a $\pm 4.6\%$ variation in the total inelastic cross section value at 13 TeV [62]. The effect of jet energy resolution is evaluated by smearing jet energies according to their estimated uncertainty. The jet energy scale is varied within one s.d. as a function of jet p_T and $|\eta|$, and the efficiency of the selection criteria is recomputed. The trigger efficiency correction factor discussed in section 5 is affected by a 2% uncertainty that is taken as a systematic uncertainty in the related source. In the mentioned sources of systematic uncertainty, both shape and normalization shifts are considered in the model. The signal yield for a given production cross section is affected by a systematic uncertainty in the measured integrated luminosity of 2.5% [63]. The effect of variation of the μ_R and μ_F scales on the signal acceptance is estimated by taking the maximum and the minimum difference with respect to the nominal acceptance when varying μ_F and μ_R each individually as well as both together up and down by a factor of two. Lastly, to estimate the signal acceptance uncertainty due to PDF uncertainties, the PDF4LHC [64] recommendation is followed, using as the uncertainty the s.d. in the acceptance for a set of 100 MC replicas of the NNPDF 3.0 set [39].

10 Results

We search for the presence of HH events in CMS data collected in the 2016 run of the LHC using the BDT discriminant trained on the SM signal simulation and artificial background data. Two-component likelihood fits to the binned BDT output distributions are performed, using the BDT distribution for the background resulting from the artificial data set described in section 8 and the signal simulations corresponding to the SM and each of the BSM benchmark points. The validation samples were used to study the dependence of both the expected limit and the compatibility of the data and background distributions on the value of the BDT discriminator used for the selection. Selecting BDT discriminator values >0.2 results in a small loss of sensitivity ($\approx$1.5%) with improved data-background

JHEP04(2019)112

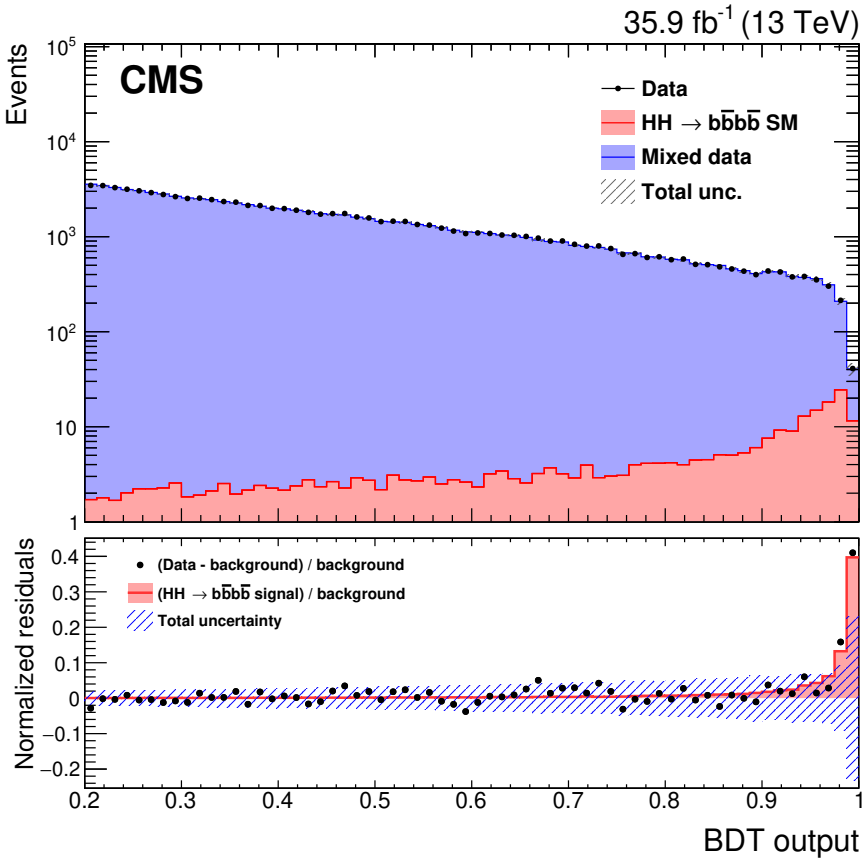

Figure 7. Results of the fit to the BDT distribution for the SM HH production signal. In the bottom panel a comparison is shown between the best fit signal and best fit background subtracted from measured data. The band, centred at zero, shows the total uncertainty.

compatibility. As a result, the 64 bins with BDT >0.2 are used to extract the limits. The fit to the SM signal is shown in figure 7 and the postfit distributions of reconstructed Higgs boson masses are shown in figure 8. Minor background contamination arising from $\mathrm{t\bar{t}H}$, ZH, $\mathrm{b\bar{b}H}$, and single Higgs boson production processes do not show a signal-like BDT distribution and their effect is found to be negligible in the selected data at our level of sensitivity.

The observed and expected 95% confidence level (CL) upper limits on the cross section for $\mathrm{pp} \to \mathrm{HH} \to \mathrm{b\bar{b}b\bar{b}}$ nonresonant production, are computed using the asymptotic approximation [65] of the $\mathrm{CL_s}$ criterion [66–68], using a test statistic based on the profile likelihood ratio (the LHC test statistic) [65]. The systematic uncertainties are treated as nuisance parameters and are profiled in the minimization. The limits are shown in table 5 together with the 1 s.d. and 2 s.d. CL intervals around the expected limits. For the SM process, the expected limit is 419 fb, which corresponds to ≈37 times the SM HH production cross section times the square of the branching fraction for the $\mathrm{H} \to \mathrm{b\bar{b}}$ decay. The observed upper limit obtained is 847 fb, which is ≈2 s.d. above the expected upper limit. This corresponds to an observed limit of 2496 fb for $\sigma(\mathrm{pp} \to \mathrm{HH})_{\mathrm{SM}}$.

JHEP04(2019)112

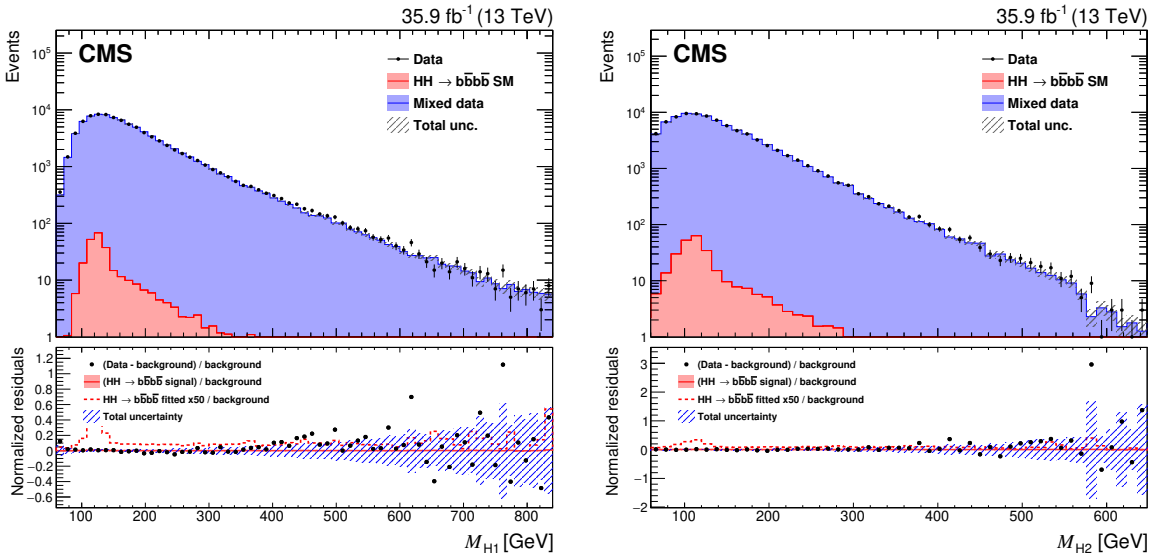

Figure 8. Post-fit distribution of M_{H_1} (left) and M_{H_2} (right). Bias correction for the background model is applied by rescaling the weight of each event using the event yield ratio between corrected and uncorrected BDT distributions.

Category	Observed	Expected	-2 s.d.	-1 s.d.	+1 s.d.	+2 s.d.
SM HH $\to$ b$\bar{\text{b}}$b$\bar{\text{b}}$	847	419	221	297	601	834

Table 5. The observed and expected upper limits on $\sigma(\text{pp} \to \text{HH} \to \text{b}\bar{\text{b}}\text{b}\bar{\text{b}})$ in the SM at 95% CL in units of fb.

We perform the procedure described above in turn on the 13 BSM benchmark models considered. The results are shown in figure 9 and reported in table 6. The difference between observed and expected limits is similar for SM and all the benchmark models. This is explained by the fact that the benchmark points use the same BDT as SM, resulting in the same background shape as an input to the fit. The background shape has a deficit of events compared to data in the last bins of the BDT distribution, as seen in figure 7. We also search for HH production with values of κ_λ in the range [-20, 20], assuming $\kappa_t = 1$, and the results are shown in figure 10. The kinematic properties vary significantly across the points in this range. We do not exclude any values of κ_λ, assuming $\kappa_t = 1$.

11 Summary

This paper presents a search for nonresonant Higgs boson pair (HH) production with both Higgs bosons decaying into b$\bar{\text{b}}$ pairs. The standard model (SM) production has been studied along with 13 beyond the SM (BSM) benchmark models, using a data set of $\sqrt{s} = 13\,\text{TeV}$ proton-proton collision events, corresponding to an integrated luminosity of $35.9\,\text{fb}^{-1}$ collected by the CMS detector during the 2016 LHC run. The analysis of events acquired by a hadronic multijet trigger includes the selection of events with 4 b-tagged jets and a classification using boosted decision trees, optimized for discovery of the SM

JHEP04(2019)112

Benchmark point	Observed	Expected	-2 s.d.	-1 s.d.	+1 s.d.	+2 s.d.
1	602	295	155	209	424	592
2	554	269	141	190	389	548
3	705	346	182	245	497	691
4	939	461	244	327	662	920
5	508	248	131	176	357	501
6	937	457	240	323	657	916
7	3510	1710	905	1210	2440	3390
8	686	336	177	238	483	674
9	529	259	136	183	373	520
10	2090	1000	527	709	1440	2010
11	1080	525	277	372	755	1050
12	1744	859	455	611	1230	1710
Box	1090	542	286	384	775	1080

Table 6. The observed and expected upper limits on the $\sigma(pp \to HH \to b\bar{b}b\bar{b})$ cross section for the 13 BSM benchmark models at 95% CL in units of fb.

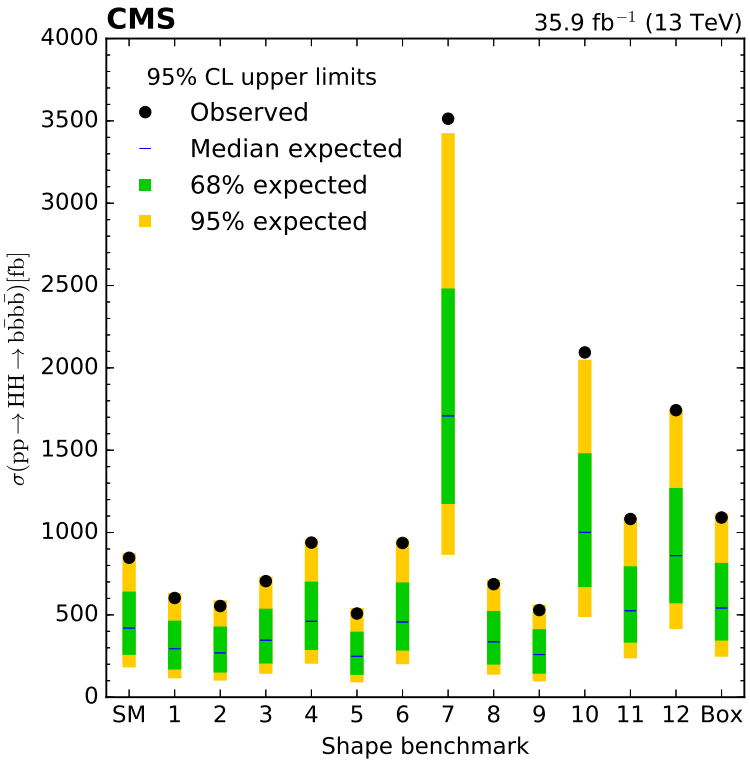

Figure 9. The observed and expected upper limits at 95% CL on the $\sigma(pp \to HH \to b\bar{b}b\bar{b})$ cross section for the 13 BSM models investigated. See table 1 for their respective parameter values.

JHEP04(2019)112

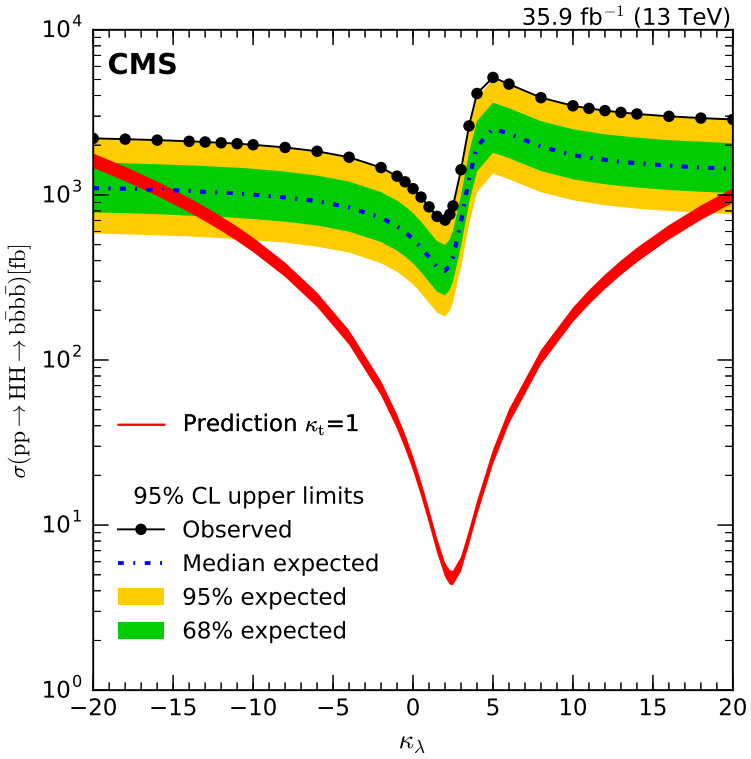

Figure 10. 95% CL cross section limits on $\sigma(pp \to HH \to b\bar{b}b\bar{b})$ for values of κ_λ in the [-20,20] range, assuming $\kappa_t = 1$; the theoretical prediction with $\kappa_t = 1$ is also shown.

HH signal. Limits at 95% confidence level on the HH production cross section times the square of the branching fraction for the Higgs boson decay to b quark pairs are extracted for the SM and each BSM model considered, using binned likelihood fits of the shape of the boosted decision tree classifier output. The background model is derived from a novel technique based on data that provides a multidimensional representation of the dominant quantum chromodynamics multijet background and also models well the overall background distribution. The expected upper limit on $\sigma(pp \to HH \to b\bar{b}b\bar{b})$ is 419 fb, corresponding to 37 times the expected value for the SM process. The observed upper limit is 847 fb. Anomalous couplings of the Higgs boson are also investigated. The upper limits extracted for the HH production cross section in the 13 BSM benchmark models range from 508 to 3513 fb.

Acknowledgments

We congratulate our colleagues in the CERN accelerator departments for the excellent performance of the LHC and thank the technical and administrative staffs at CERN and at other CMS institutes for their contributions to the success of the CMS effort. In addition, we gratefully acknowledge the computing centres and personnel of the Worldwide LHC Computing Grid for delivering so effectively the computing infrastructure essential to our analyses. Finally, we acknowledge the enduring support for the construction and operation

JHEP04(2019)112

of the LHC and the CMS detector provided by the following funding agencies: BMBWF and FWF (Austria); FNRS and FWO (Belgium); CNPq, CAPES, FAPERJ, FAPERGS, and FAPESP (Brazil); MES (Bulgaria); CERN; CAS, MoST, and NSFC (China); COLCIENCIAS (Colombia); MSES and CSF (Croatia); RPF (Cyprus); SENESCYT (Ecuador); MoER, ERC IUT, and ERDF (Estonia); Academy of Finland, MEC, and HIP (Finland); CEA and CNRS/IN2P3 (France); BMBF, DFG, and HGF (Germany); GSRT (Greece); NKFIA (Hungary); DAE and DST (India); IPM (Iran); SFI (Ireland); INFN (Italy); MSIP and NRF (Republic of Korea); MES (Latvia); LAS (Lithuania); MOE and UM (Malaysia); BUAP, CINVESTAV, CONACYT, LNS, SEP, and UASLP-FAI (Mexico); MOS (Montenegro); MBIE (New Zealand); PAEC (Pakistan); MSHE and NSC (Poland); FCT (Portugal); JINR (Dubna); MON, RosAtom, RAS, RFBR, and NRC KI (Russia); MESTD (Serbia); SEIDI, CPAN, PCTI, and FEDER (Spain); MOSTR (Sri Lanka); Swiss Funding Agencies (Switzerland); MST (Taipei); ThEPCenter, IPST, STAR, and NSTDA (Thailand); TUBITAK and TAEK (Turkey); NASU and SFFR (Ukraine); STFC (United Kingdom); DOE and NSF (U.S.A.).

Individuals have received support from the Marie-Curie programme and the European Research Council and Horizon 2020 Grant, contract No. 675440 (European Union); the Leventis Foundation; the A.P. Sloan Foundation; the Alexander von Humboldt Foundation; the Belgian Federal Science Policy Office; the Fonds pour la Formation à la Recherche dans l'Industrie et dans l'Agriculture (FRIA-Belgium); the Agentschap voor Innovatie door Wetenschap en Technologie (IWT-Belgium); the F.R.S.-FNRS and FWO (Belgium) under the "Excellence of Science — EOS" — be.h project n. 30820817; the Ministry of Education, Youth and Sports (MEYS) of the Czech Republic; the Lendület ("Momentum") Programme and the János Bolyai Research Scholarship of the Hungarian Academy of Sciences, the New National Excellence Program ÚNKP, the NKFIA research grants 123842, 123959, 124845, 124850 and 125105 (Hungary); the Council of Science and Industrial Research, India; the HOMING PLUS programme of the Foundation for Polish Science, cofinanced from European Union, Regional Development Fund, the Mobility Plus programme of the Ministry of Science and Higher Education, the National Science Center (Poland), contracts Harmonia 2014/14/M/ST2/00428, Opus 2014/13/B/ST2/02543, 2014/15/B/ST2/03998, and 2015/19/B/ST2/02861, Sonata-bis 2012/07/E/ST2/01406; the National Priorities Research Program by Qatar National Research Fund; the Programa Estatal de Fomento de la Investigación Científica y Técnica de Excelencia María de Maeztu, grant MDM-2015-0509 and the Programa Severo Ochoa del Principado de Asturias; the Thalis and Aristeia programmes cofinanced by EU-ESF and the Greek NSRF; the Rachadapisek Sompot Fund for Postdoctoral Fellowship, Chulalongkorn University and the Chulalongkorn Academic into Its 2nd Century Project Advancement Project (Thailand); the Welch Foundation, contract C-1845; and the Weston Havens Foundation (U.S.A.).

A Supplemental material

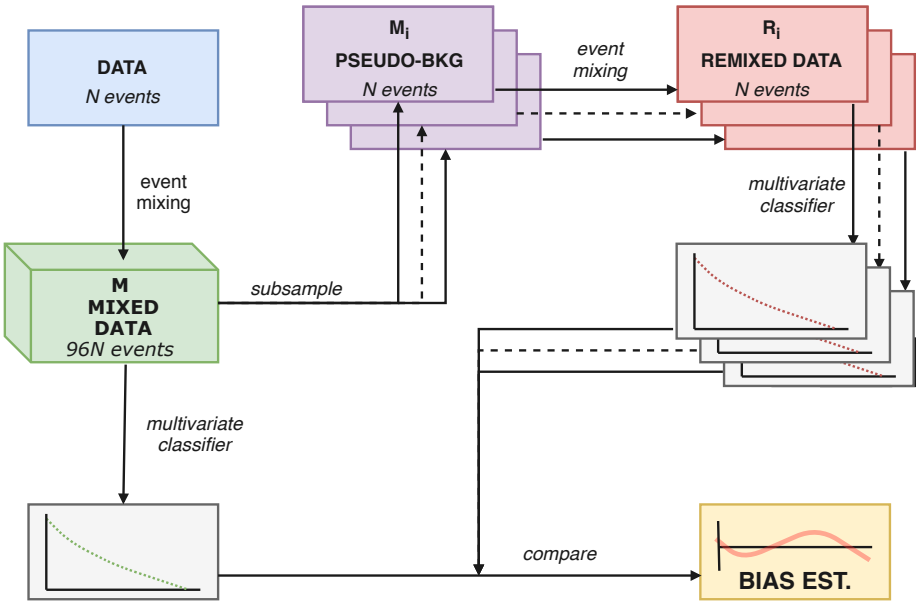

Figure 11. Diagram describing the procedure used to estimate the background bias correction. All possible combinations of mixed hemispheres except those used for training are added together to create a large sample M of $96N$ events from which we repeatedly subsample without replacement 200 replicas M_i of N events. The hemisphere mixing procedure is then carried out again for each of this replicas to produce a set of re-mixed data replicas R_i. The trained multivariate classifier trained is then evaluated over all the events of M and each R_i. and the histograms of the classifier output are compared to obtain a the differences for each of the replicas. The median difference is taken as bias correction.

JHEP04(2019)112

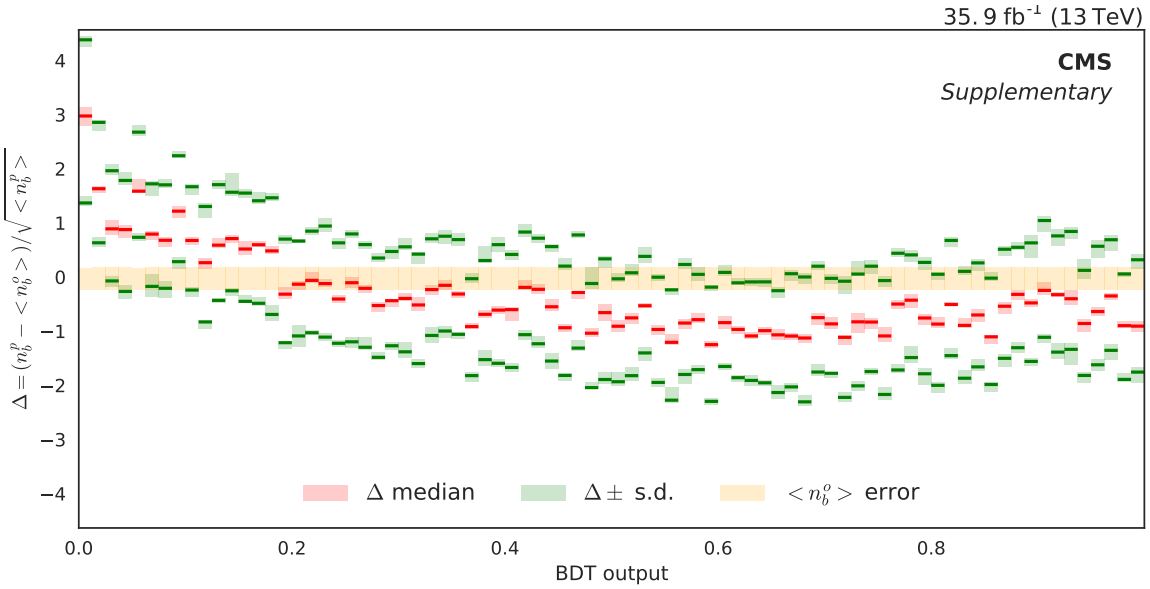

Figure 12. Bias estimation by resampling, in relative units of the statistical uncertainty of the predicted background, used to correct the background estimation. The median (red line) and the upper and lower one s.d. quantiles (green lines) have been computed from 200 subsamples of the re-mixed data comparing the predicted background n_b^p with the observed n_b^o. The variability due to the limited number of subsamples is estimated by bootstrap and it is shown for each estimation using a coloured shadow around the quantile estimation. The light yellow shadow represents the uncertainty due to the limited statistics of the reference observed sample. The separation between the one s.d. quantiles is compatible with the expected variance if the estimation was Poisson or Gaussian distributed.

JHEP04(2019)112

References

[1] ATLAS collaboration, *Observation of a new particle in the search for the Standard Model Higgs boson with the ATLAS detector at the LHC*, *Phys. Lett.* **B 716** (2012) 1 [arXiv:1207.7214] [INSPIRE].

[2] CMS collaboration, *Observation of a new boson at a mass of* 125 *GeV with the CMS experiment at the LHC*, *Phys. Lett.* **B 716** (2012) 30 [arXiv:1207.7235] [INSPIRE].

[3] CMS collaboration, *Observation of a new boson with mass near* 125 *GeV in pp collisions at* $\sqrt{s} = 7$ *and* 8 *TeV*, *JHEP* **06** (2013) 081 [arXiv:1303.4571] [INSPIRE].

[4] ATLAS and CMS collaborations, *Measurements of the Higgs boson production and decay rates and constraints on its couplings from a combined ATLAS and CMS analysis of the LHC pp collision data at* $\sqrt{s} = 7$ *and* 8 *TeV*, *JHEP* **08** (2016) 045 [arXiv:1606.02266] [INSPIRE].

[5] ATLAS and CMS collaborations, *Combined measurement of the Higgs boson mass in pp collisions at* $\sqrt{s} = 7$ *and* 8 *TeV with the ATLAS and CMS experiments*, *Phys. Rev. Lett.* **114** (2015) 191803 [arXiv:1503.07589] [INSPIRE].

[6] C.O. Dib, R. Rosenfeld and A. Zerwekh, *Double Higgs production and quadratic divergence cancellation in little Higgs models with T parity*, *JHEP* **05** (2006) 074 [hep-ph/0509179] [INSPIRE].

[7] R. Grober and M. Muhlleitner, *Composite Higgs boson pair production at the LHC*, *JHEP* **06** (2011) 020 [arXiv:1012.1562] [INSPIRE].

[8] R. Contino, M. Ghezzi, M. Moretti, G. Panico, F. Piccinini and A. Wulzer, *Anomalous couplings in double Higgs production*, *JHEP* **08** (2012) 154 [arXiv:1205.5444] [INSPIRE].

[9] M.J. Dolan, C. Englert and M. Spannowsky, *New physics in LHC Higgs boson pair production*, *Phys. Rev.* **D 87** (2013) 055002 [arXiv:1210.8166] [INSPIRE].

[10] S. Dawson, A. Ismail and I. Low, *What's in the loop? The anatomy of double Higgs production*, *Phys. Rev.* **D 91** (2015) 115008 [arXiv:1504.05596] [INSPIRE].

[11] J. Baglio, A. Djouadi, R. Gröber, M.M. Mühlleitner, J. Quevillon and M. Spira, *The measurement of the Higgs self-coupling at the LHC: theoretical status*, *JHEP* **04** (2013) 151 [arXiv:1212.5581] [INSPIRE].

[12] CMS collaboration, *Measurements of properties of the Higgs boson decaying into the four-lepton final state in pp collisions at* $\sqrt{s} = 13$ *TeV*, *JHEP* **11** (2017) 047 [arXiv:1706.09936] [INSPIRE].

[13] LHC Higgs Cross Section Working Group collaboration, *Handbook of LHC Higgs cross sections: 4. Deciphering the nature of the Higgs sector*, arXiv:1610.07922 [INSPIRE].

[14] D. de Florian and J. Mazzitelli, *Higgs boson pair production at next-to-next-to-leading order in QCD*, *Phys. Rev. Lett.* **111** (2013) 201801 [arXiv:1309.6594] [INSPIRE].

[15] S. Dawson, S. Dittmaier and M. Spira, *Neutral Higgs boson pair production at hadron colliders: QCD corrections*, *Phys. Rev.* **D 58** (1998) 115012 [hep-ph/9805244] [INSPIRE].

JHEP04(2019)112

[16] S. Borowka et al., *Higgs boson pair production in gluon fusion at next-to-leading order with full top-quark mass dependence*, *Phys. Rev. Lett.* **117** (2016) 012001 [*Erratum ibid.* **117** (2016) 079901] [arXiv:1604.06447] [INSPIRE].

[17] D. de Florian and J. Mazzitelli, *Higgs pair production at next-to-next-to-leading logarithmic accuracy at the LHC*, *JHEP* **09** (2015) 053 [arXiv:1505.07122] [INSPIRE].

[18] CMS collaboration, *Search for Higgs boson pair production in events with two bottom quarks and two tau leptons in proton-proton collisions at* $\sqrt{s} = 13$ *TeV*, *Phys. Lett.* **B 778** (2018) 101 [arXiv:1707.02909] [INSPIRE].

[19] ATLAS collaboration, *Search for pair production of Higgs bosons in the* $b\bar{b}b\bar{b}$ *final state using proton-proton collisions at* $\sqrt{s} = 13$ *TeV with the ATLAS detector*, *JHEP* **01** (2019) 030 [arXiv:1804.06174] [INSPIRE].

[20] A. Carvalho et al., *Analytical parametrization and shape classification of anomalous HH production in the EFT approach*, arXiv:1608.06578 [INSPIRE].

[21] ATLAS collaboration, *Search for Higgs boson pair production in the* $b\bar{b}b\bar{b}$ *final state from pp collisions at* $\sqrt{s} = 8$ *TeV with the ATLAS detector*, *Eur. Phys. J.* **C 75** (2015) 412 [arXiv:1506.00285] [INSPIRE].

[22] CMS collaboration, *Search for Higgs boson pair production in the* $\mathrm{bb}\tau\tau$ *final state in proton-proton collisions at* $\sqrt{s} = 8$ *TeV*, *Phys. Rev.* **D 96** (2017) 072004 [arXiv:1707.00350] [INSPIRE].

[23] CMS collaboration, *Search for resonant and nonresonant Higgs boson pair production in the* $\mathrm{bb}\ell\nu\ell\nu$ *final state in proton-proton collisions at* $\sqrt{s} = 13$ *TeV*, *JHEP* **01** (2018) 054 [arXiv:1708.04188] [INSPIRE].

[24] ATLAS collaboration, *Search for Higgs boson pair production in the* $b\bar{b}WW^*$ *decay mode at* $\sqrt{s} = 13$ *TeV with the ATLAS detector*, submitted to *JHEP* [arXiv:1811.04671] [INSPIRE].

[25] ATLAS collaboration, *Search for resonant and non-resonant Higgs boson pair production in the* $b\bar{b}\tau^+\tau^-$ *decay channel in pp collisions at* $\sqrt{s} = 13$ *TeV with the ATLAS detector*, *Phys. Rev. Lett.* **121** (2018) 191801 [*Erratum ibid.* **122** (2019) 089901] [arXiv:1808.00336] [INSPIRE].

[26] CMS collaboration, *Search for Higgs boson pair production in the* $\gamma\gamma\mathrm{b\bar{b}}$ *final state in pp collisions at* $\sqrt{s} = 13$ *TeV*, *Phys. Lett.* **B 788** (2019) 7 [arXiv:1806.00408] [INSPIRE].

[27] ATLAS collaboration, *Search for Higgs boson pair production in the* $\gamma\gamma b\bar{b}$ *final state with 13 TeV pp collision data collected by the ATLAS experiment*, *JHEP* **11** (2018) 040 [arXiv:1807.04873] [INSPIRE].

[28] ATLAS collaboration, *Search for Higgs boson pair production in the* $\gamma\gamma WW^*$ *channel using pp collision data recorded at* $\sqrt{s} = 13$ *TeV with the ATLAS detector*, *Eur. Phys. J.* **C 78** (2018) 1007 [arXiv:1807.08567] [INSPIRE].

[29] ATLAS collaboration, *Search for Higgs boson pair production in the* $WW^{(*)}WW^{(*)}$ *decay channel using ATLAS data recorded at* $\sqrt{s} = 13$ *TeV*, submitted to *JHEP* [arXiv:1811.11028] [INSPIRE].

[30] CMS collaboration, *Search for production of Higgs boson pairs in the four b quark final state using large-area jets in proton-proton collisions at* $\sqrt{s} = 13$ *TeV*, *JHEP* **01** (2019) 040 [arXiv:1808.01473] [INSPIRE].

[31] A. Falkowski, *Effective field theory approach to LHC Higgs data*, *Pramana* **87** (2016) 39 [arXiv:1505.00046] [INSPIRE].

JHEP04(2019)112

[32] T. Corbett, O.J.P. Eboli, D. Goncalves, J. Gonzalez-Fraile, T. Plehn and M. Rauch, *The Higgs legacy of the LHC run I*, *JHEP* **08** (2015) 156 [arXiv:1505.05516] [INSPIRE].

[33] A. Carvalho, M. Dall'Osso, T. Dorigo, F. Goertz, C.A. Gottardo and M. Tosi, *Higgs pair production: Choosing benchmarks with cluster analysis*, *JHEP* **04** (2016) 126 [arXiv:1507.02245] [INSPIRE].

[34] CMS collaboration, *The CMS trigger system*, 2017 *JINST* **12** P01020 [arXiv:1609.02366] [INSPIRE].

[35] CMS collaboration, *The CMS experiment at the CERN LHC*, 2008 *JINST* **3** S08004 [INSPIRE].

[36] CMS collaboration, *Identification of heavy-flavour jets with the CMS detector in pp collisions at* 13 *TeV*, 2018 *JINST* **13** P05011 [arXiv:1712.07158] [INSPIRE].

[37] B. Hespel, D. Lopez-Val and E. Vryonidou, *Higgs pair production via gluon fusion in the Two-Higgs-Doublet Model*, *JHEP* **09** (2014) 124 [arXiv:1407.0281] [INSPIRE].

[38] J. Alwall et al., *The automated computation of tree-level and next-to-leading order differential cross sections and their matching to parton shower simulations*, *JHEP* **07** (2014) 079 [arXiv:1405.0301] [INSPIRE].

[39] NNPDF collaboration, *Parton distributions for the LHC Run II*, *JHEP* **04** (2015) 040 [arXiv:1410.8849] [INSPIRE].

[40] A. Carvalho, F. Goertz, K. Mimasu, M. Gouzevitch and A. Aggarwal, *On the reinterpretation of non-resonant searches for Higgs boson pairs*, arXiv:1710.08261 [INSPIRE].

[41] T. Sjöstrand et al., *An introduction to PYTHIA 8.2*, *Comput. Phys. Commun.* **191** (2015) 159 [arXiv:1410.3012] [INSPIRE].

[42] J. Alwall et al., *Comparative study of various algorithms for the merging of parton showers and matrix elements in hadronic collisions*, *Eur. Phys. J.* **C 53** (2008) 473 [arXiv:0706.2569] [INSPIRE].

[43] P. Nason, *A new method for combining NLO QCD with shower Monte Carlo algorithms*, *JHEP* **11** (2004) 040 [hep-ph/0409146] [INSPIRE].

[44] S. Frixione, P. Nason and C. Oleari, *Matching NLO QCD computations with parton shower simulations: the POWHEG method*, *JHEP* **11** (2007) 070 [arXiv:0709.2092] [INSPIRE].

[45] S. Alioli, P. Nason, C. Oleari and E. Re, *A general framework for implementing NLO calculations in shower Monte Carlo programs: the POWHEG BOX*, *JHEP* **06** (2010) 043 [arXiv:1002.2581] [INSPIRE].

[46] J.M. Campbell, R.K. Ellis, P. Nason and E. Re, *Top-pair production and decay at NLO matched with parton showers*, *JHEP* **04** (2015) 114 [arXiv:1412.1828] [INSPIRE].

[47] S. Alioli, P. Nason, C. Oleari and E. Re, *NLO single-top production matched with shower in POWHEG: s- and t-channel contributions*, *JHEP* **09** (2009) 111 [*Erratum ibid.* **02** (2010) 011] [arXiv:0907.4076] [INSPIRE].

[48] H.B. Hartanto, B. Jager, L. Reina and D. Wackeroth, *Higgs boson production in association with top quarks in the POWHEG BOX*, *Phys. Rev.* **D 91** (2015) 094003 [arXiv:1501.04498] [INSPIRE].

[49] E. Bagnaschi, G. Degrassi, P. Slavich and A. Vicini, *Higgs production via gluon fusion in the POWHEG approach in the SM and in the MSSM*, *JHEP* **02** (2012) 088 [arXiv:1111.2854] [INSPIRE].

JHEP04(2019)112

[50] G. Luisoni, P. Nason, C. Oleari and F. Tramontano, *$HW^{\pm}/HZ + 0$ and 1 jet at NLO with the POWHEG BOX interfaced to GoSam and their merging within MiNLO*, *JHEP* **10** (2013) 083 [arXiv:1306.2542] [INSPIRE].

[51] CMS collaboration, *Investigations of the impact of the parton shower tuning in Pythia 8 in the modelling of $\mathrm{t\bar{t}}$ at $\sqrt{s} = 8$ and 13 TeV*, CMS-PAS-TOP-16-021.

[52] CMS collaboration, *Event generator tunes obtained from underlying event and multiparton scattering measurements*, *Eur. Phys. J.* **C 76** (2016) 155 [arXiv:1512.00815] [INSPIRE].

[53] A. Buckley et al., *LHAPDF6: parton density access in the LHC precision era*, *Eur. Phys. J.* **C 75** (2015) 132 [arXiv:1412.7420] [INSPIRE].

[54] GEANT4 collaboration, GEANT4 — *a simulation toolkit*, *Nucl. Instrum. Meth.* **A 506** (2003) 250 [INSPIRE].

[55] CMS collaboration, *Particle-flow reconstruction and global event description with the CMS detector*, 2017 *JINST* **12** P10003 [arXiv:1706.04965] [INSPIRE].

[56] M. Cacciari, G.P. Salam and G. Soyez, *The anti-k_{T} jet clustering algorithm*, *JHEP* **04** (2008) 063 [arXiv:0802.1189] [INSPIRE].

[57] M. Cacciari, G.P. Salam and G. Soyez, *FastJet user manual*, *Eur. Phys. J.* **C 72** (2012) 1896 [arXiv:1111.6097] [INSPIRE].

[58] CMS collaboration, *Jet energy scale and resolution in the CMS experiment in pp collisions at 8 TeV*, 2017 *JINST* **12** P02014 [arXiv:1607.03663] [INSPIRE].

[59] CMS collaboration, *Pileup jet identification*, CMS-PAS-JME-13-005.

[60] T. Chen and C. Guestrin, *XGBoost: A scalable tree boosting system*, in *Proceedings of the 22nd ACM SIGKDD International Conference on Knowledge Discovery and Data Mining, KDD '16*, ACM, New York, NY, U.S.A. (2016) [DOI:10.1145/2939672.2939785].

[61] P. De Castro Manzano et al., *Hemisphere mixing: a fully data-driven model of QCD multijet backgrounds for LHC searches*, PoS(EPS-HEP2017)370 (2017) [arXiv:1712.02538] [INSPIRE].

[62] CMS collaboration, *Measurement of the inelastic proton-proton cross section at $\sqrt{s} = 13$ TeV*, *JHEP* **07** (2018) 161 [arXiv:1802.02613] [INSPIRE].

[63] CMS collaboration, *CMS luminosity measurements or the 2016 data taking period*, CMS-PAS-LUM-17-001.

[64] J. Butterworth et al., *PDF4LHC recommendations for LHC Run II*, *J. Phys.* **G 43** (2016) 023001 [arXiv:1510.03865] [INSPIRE].

[65] G. Cowan, K. Cranmer, E. Gross and O. Vitells, *Asymptotic formulae for likelihood-based tests of new physics*, *Eur. Phys. J.* **C 71** (2011) 1554 [*Erratum ibid.* **C 73** (2013) 2501] [arXiv:1007.1727] [INSPIRE].

[66] A.L. Read, *Presentation of search results: The CL_s technique*, *J. Phys.* **G 28** (2002) 2693 [INSPIRE].

[67] T. Junk, *Confidence level computation for combining searches with small statistics*, *Nucl. Instrum. Meth.* **A 434** (1999) 435 [hep-ex/9902006] [INSPIRE].

[68] ATLAS and CMS collaborations and The LHC HIGGS Combination Group, *Procedure for the LHC Higgs boson search combination in Summer 2011*, CMS-NOTE-2011-005, ATL-PHYS-PUB-2011-11.

JHEP04(2019)112

The CMS collaboration

Yerevan Physics Institute, Yerevan, Armenia

A.M. Sirunyan, A. Tumasyan

Institut für Hochenergiephysik, Wien, Austria

W. Adam, F. Ambrogi, E. Asilar, T. Bergauer, J. Brandstetter, M. Dragicevic, J. Erö, A. Escalante Del Valle, M. Flechl, R. Frühwirth[1], V.M. Ghete, J. Hrubec, M. Jeitler[1], N. Krammer, I. Krätschmer, D. Liko, T. Madlener, I. Mikulec, N. Rad, H. Rohringer, J. Schieck[1], R. Schöfbeck, M. Spanring, D. Spitzbart, A. Taurok, W. Waltenberger, J. Wittmann, C.-E. Wulz[1], M. Zarucki

Institute for Nuclear Problems, Minsk, Belarus

V. Chekhovsky, V. Mossolov, J. Suarez Gonzalez

Universiteit Antwerpen, Antwerpen, Belgium

E.A. De Wolf, D. Di Croce, X. Janssen, J. Lauwers, M. Pieters, H. Van Haevermaet, P. Van Mechelen, N. Van Remortel

Vrije Universiteit Brussel, Brussel, Belgium

S. Abu Zeid, F. Blekman, J. D'Hondt, J. De Clercq, K. Deroover, G. Flouris, D. Lontkovskyi, S. Lowette, I. Marchesini, S. Moortgat, L. Moreels, Q. Python, K. Skovpen, S. Tavernier, W. Van Doninck, P. Van Mulders, I. Van Parijs

Université Libre de Bruxelles, Bruxelles, Belgium

D. Beghin, B. Bilin, H. Brun, B. Clerbaux, G. De Lentdecker, H. Delannoy, B. Dorney, G. Fasanella, L. Favart, R. Goldouzian, A. Grebenyuk, A.K. Kalsi, T. Lenzi, J. Luetic, N. Postiau, E. Starling, L. Thomas, C. Vander Velde, P. Vanlaer, D. Vannerom, Q. Wang

Ghent University, Ghent, Belgium

T. Cornelis, D. Dobur, A. Fagot, M. Gul, I. Khvastunov[2], D. Poyraz, C. Roskas, D. Trocino, M. Tytgat, W. Verbeke, B. Vermassen, M. Vit, N. Zaganidis

Université Catholique de Louvain, Louvain-la-Neuve, Belgium

H. Bakhshiansohi, O. Bondu, S. Brochet, G. Bruno, C. Caputo, P. David, C. Delaere, M. Delcourt, A. Giammanco, G. Krintiras, V. Lemaitre, A. Magitteri, K. Piotrzkowski, A. Saggio, M. Vidal Marono, S. Wertz, J. Zobec

Centro Brasileiro de Pesquisas Fisicas, Rio de Janeiro, Brazil

F.L. Alves, G.A. Alves, M. Correa Martins Junior, G. Correia Silva, C. Hensel, A. Moraes, M.E. Pol, P. Rebello Teles

Universidade do Estado do Rio de Janeiro, Rio de Janeiro, Brazil

E. Belchior Batista Das Chagas, W. Carvalho, J. Chinellato[3], E. Coelho, E.M. Da Costa, G.G. Da Silveira[4], D. De Jesus Damiao, C. De Oliveira Martins, S. Fonseca De Souza, H. Malbouisson, D. Matos Figueiredo, M. Melo De Almeida, C. Mora Herrera, L. Mundim, H. Nogima, W.L. Prado Da Silva, L.J. Sanchez Rosas, A. Santoro, A. Sznajder, M. Thiel, E.J. Tonelli Manganote[3], F. Torres Da Silva De Araujo, A. Vilela Pereira

JHEP04(2019)112

Universidade Estadual Paulista [a], Universidade Federal do ABC [b], São Paulo, Brazil

S. Ahuja[a], C.A. Bernardes[a], L. Calligaris[a], T.R. Fernandez Perez Tomei[a], E.M. Gregores[b], P.G. Mercadante[b], S.F. Novaes[a], SandraS. Padula[a]

Institute for Nuclear Research and Nuclear Energy, Bulgarian Academy of Sciences, Sofia, Bulgaria

A. Aleksandrov, R. Hadjiiska, P. Iaydjiev, A. Marinov, M. Misheva, M. Rodozov, M. Shopova, G. Sultanov

University of Sofia, Sofia, Bulgaria

A. Dimitrov, L. Litov, B. Pavlov, P. Petkov

Beihang University, Beijing, China

W. Fang[5], X. Gao[5], L. Yuan

Institute of High Energy Physics, Beijing, China

M. Ahmad, J.G. Bian, G.M. Chen, H.S. Chen, M. Chen, Y. Chen, C.H. Jiang, D. Leggat, H. Liao, Z. Liu, F. Romeo, S.M. Shaheen[6], A. Spiezia, J. Tao, Z. Wang, E. Yazgan, H. Zhang, S. Zhang[6], J. Zhao

State Key Laboratory of Nuclear Physics and Technology, Peking University, Beijing, China

Y. Ban, G. Chen, A. Levin, J. Li, L. Li, Q. Li, Y. Mao, S.J. Qian, D. Wang

Tsinghua University, Beijing, China

Y. Wang

Universidad de Los Andes, Bogota, Colombia

C. Avila, A. Cabrera, C.A. Carrillo Montoya, L.F. Chaparro Sierra, C. Florez, C.F. González Hernández, M.A. Segura Delgado

University of Split, Faculty of Electrical Engineering, Mechanical Engineering and Naval Architecture, Split, Croatia

B. Courbon, N. Godinovic, D. Lelas, I. Puljak, T. Sculac

University of Split, Faculty of Science, Split, Croatia

Z. Antunovic, M. Kovac

Institute Rudjer Boskovic, Zagreb, Croatia

V. Brigljevic, D. Ferencek, K. Kadija, B. Mesic, A. Starodumov[7], T. Susa

University of Cyprus, Nicosia, Cyprus

M.W. Ather, A. Attikis, M. Kolosova, G. Mavromanolakis, J. Mousa, C. Nicolaou, F. Ptochos, P.A. Razis, H. Rykaczewski

Charles University, Prague, Czech Republic

M. Finger[8], M. Finger Jr.[8]

JHEP04(2019)112

Escuela Politecnica Nacional, Quito, Ecuador

E. Ayala

Universidad San Francisco de Quito, Quito, Ecuador

E. Carrera Jarrin

Academy of Scientific Research and Technology of the Arab Republic of Egypt, Egyptian Network of High Energy Physics, Cairo, Egypt

H. Abdalla[9], A.A. Abdelalim[10,11], A. Mohamed[11]

National Institute of Chemical Physics and Biophysics, Tallinn, Estonia

S. Bhowmik, A. Carvalho Antunes De Oliveira, R.K. Dewanjee, K. Ehataht, M. Kadastik, M. Raidal, C. Veelken

Department of Physics, University of Helsinki, Helsinki, Finland

P. Eerola, H. Kirschenmann, J. Pekkanen, M. Voutilainen

Helsinki Institute of Physics, Helsinki, Finland

J. Havukainen, J.K. Heikkilä, T. Järvinen, V. Karimäki, R. Kinnunen, T. Lampén, K. Lassila-Perini, S. Laurila, S. Lehti, T. Lindén, P. Luukka, T. Mäenpää, H. Siikonen, E. Tuominen, J. Tuominiemi

Lappeenranta University of Technology, Lappeenranta, Finland

T. Tuuva

IRFU, CEA, Université Paris-Saclay, Gif-sur-Yvette, France

M. Besancon, F. Couderc, M. Dejardin, D. Denegri, J.L. Faure, F. Ferri, S. Ganjour, A. Givernaud, P. Gras, G. Hamel de Monchenault, P. Jarry, C. Leloup, E. Locci, J. Malcles, G. Negro, J. Rander, A. Rosowsky, M.Ö. Sahin, M. Titov

Laboratoire Leprince-Ringuet, Ecole polytechnique, CNRS/IN2P3, Université Paris-Saclay, Palaiseau, France

A. Abdulsalam[12], C. Amendola, I. Antropov, F. Beaudette, P. Busson, C. Charlot, R. Granier de Cassagnac, I. Kucher, A. Lobanov, J. Martin Blanco, C. Martin Perez, M. Nguyen, C. Ochando, G. Ortona, P. Paganini, P. Pigard, J. Rembser, R. Salerno, J.B. Sauvan, Y. Sirois, A.G. Stahl Leiton, A. Zabi, A. Zghiche

Université de Strasbourg, CNRS, IPHC UMR 7178, Strasbourg, France

J.-L. Agram[13], J. Andrea, D. Bloch, J.-M. Brom, E.C. Chabert, V. Cherepanov, C. Collard, E. Conte[13], J.-C. Fontaine[13], D. Gelé, U. Goerlach, M. Jansová, A.-C. Le Bihan, N. Tonon, P. Van Hove

Centre de Calcul de l'Institut National de Physique Nucleaire et de Physique des Particules, CNRS/IN2P3, Villeurbanne, France

S. Gadrat

JHEP04(2019)112

Université de Lyon, Université Claude Bernard Lyon 1, CNRS-IN2P3, Institut de Physique Nucléaire de Lyon, Villeurbanne, France
S. Beauceron, C. Bernet, G. Boudoul, N. Chanon, R. Chierici, D. Contardo, P. Depasse, H. El Mamouni, J. Fay, L. Finco, S. Gascon, M. Gouzevitch, G. Grenier, B. Ille, F. Lagarde, I.B. Laktineh, H. Lattaud, M. Lethuillier, L. Mirabito, S. Perries, A. Popov[14], V. Sordini, G. Touquet, M. Vander Donckt, S. Viret

Georgian Technical University, Tbilisi, Georgia
A. Khvedelidze[8]

Tbilisi State University, Tbilisi, Georgia
Z. Tsamalaidze[8]

RWTH Aachen University, I. Physikalisches Institut, Aachen, Germany
C. Autermann, L. Feld, M.K. Kiesel, K. Klein, M. Lipinski, M. Preuten, M.P. Rauch, C. Schomakers, J. Schulz, M. Teroerde, B. Wittmer

RWTH Aachen University, III. Physikalisches Institut A, Aachen, Germany
A. Albert, D. Duchardt, M. Erdmann, S. Erdweg, T. Esch, R. Fischer, S. Ghosh, A. Güth, T. Hebbeker, C. Heidemann, K. Hoepfner, H. Keller, L. Mastrolorenzo, M. Merschmeyer, A. Meyer, P. Millet, S. Mukherjee, T. Pook, M. Radziej, H. Reithler, M. Rieger, A. Schmidt, D. Teyssier, S. Thüer

RWTH Aachen University, III. Physikalisches Institut B, Aachen, Germany
G. Flügge, O. Hlushchenko, T. Kress, T. Müller, A. Nehrkorn, A. Nowack, C. Pistone, O. Pooth, D. Roy, H. Sert, A. Stahl[15]

Deutsches Elektronen-Synchrotron, Hamburg, Germany
M. Aldaya Martin, T. Arndt, C. Asawatangtrakuldee, I. Babounikau, K. Beernaert, O. Behnke, U. Behrens, A. Bermúdez Martínez, D. Bertsche, A.A. Bin Anuar, K. Borras[16], V. Botta, A. Campbell, P. Connor, C. Contreras-Campana, V. Danilov, A. De Wit, M.M. Defranchis, C. Diez Pardos, D. Domínguez Damiani, G. Eckerlin, T. Eichhorn, A. Elwood, E. Eren, E. Gallo[17], A. Geiser, J.M. Grados Luyando, A. Grohsjean, M. Guthoff, M. Haranko, A. Harb, J. Hauk, H. Jung, M. Kasemann, J. Keaveney, C. Kleinwort, J. Knolle, D. Krücker, W. Lange, A. Lelek, T. Lenz, J. Leonard, K. Lipka, W. Lohmann[18], R. Mankel, I.-A. Melzer-Pellmann, A.B. Meyer, M. Meyer, M. Missiroli, G. Mittag, J. Mnich, V. Myronenko, S.K. Pflitsch, D. Pitzl, A. Raspereza, M. Savitskyi, P. Saxena, P. Schütze, C. Schwanenberger, R. Shevchenko, A. Singh, H. Tholen, O. Turkot, A. Vagnerini, G.P. Van Onsem, R. Walsh, Y. Wen, K. Wichmann, C. Wissing, O. Zenaiev

University of Hamburg, Hamburg, Germany
R. Aggleton, S. Bein, L. Benato, A. Benecke, V. Blobel, T. Dreyer, A. Ebrahimi, E. Garutti, D. Gonzalez, P. Gunnellini, J. Haller, A. Hinzmann, A. Karavdina, G. Kasieczka, R. Klanner, R. Kogler, N. Kovalchuk, S. Kurz, V. Kutzner, J. Lange, D. Marconi, J. Multhaup, M. Niedziela, C.E.N. Niemeyer, D. Nowatschin, A. Perieanu, A. Reimers, O. Rieger, C. Scharf, P. Schleper, S. Schumann, J. Schwandt, J. Sonneveld, H. Stadie, G. Steinbrück, F.M. Stober, M. Stöver, A. Vanhoefer, B. Vormwald, I. Zoi

JHEP04(2019)112

Karlsruher Institut fuer Technologie, Karlsruhe, Germany
M. Akbiyik, C. Barth, M. Baselga, S. Baur, E. Butz, R. Caspart, T. Chwalek, F. Colombo, W. De Boer, A. Dierlamm, K. El Morabit, N. Faltermann, B. Freund, M. Giffels, M.A. Harrendorf, F. Hartmann[15], S.M. Heindl, U. Husemann, I. Katkov[14], S. Kudella, S. Mitra, M.U. Mozer, Th. Müller, M. Musich, M. Plagge, G. Quast, K. Rabbertz, M. Schröder, I. Shvetsov, H.J. Simonis, R. Ulrich, S. Wayand, M. Weber, T. Weiler, C. Wöhrmann, R. Wolf

Institute of Nuclear and Particle Physics (INPP), NCSR Demokritos, Aghia Paraskevi, Greece
G. Anagnostou, G. Daskalakis, T. Geralis, A. Kyriakis, D. Loukas, G. Paspalaki

National and Kapodistrian University of Athens, Athens, Greece
G. Karathanasis, P. Kontaxakis, A. Panagiotou, I. Papavergou, N. Saoulidou, E. Tziaferi, K. Vellidis

National Technical University of Athens, Athens, Greece
K. Kousouris, I. Papakrivopoulos, G. Tsipolitis

University of Ioánnina, Ioánnina, Greece
I. Evangelou, C. Foudas, P. Gianneios, P. Katsoulis, P. Kokkas, S. Mallios, N. Manthos, I. Papadopoulos, E. Paradas, J. Strologas, F.A. Triantis, D. Tsitsonis

MTA-ELTE Lendület CMS Particle and Nuclear Physics Group, Eötvös Loránd University, Budapest, Hungary
M. Bartók[19], M. Csanad, N. Filipovic, P. Major, M.I. Nagy, G. Pasztor, O. Surányi, G.I. Veres

Wigner Research Centre for Physics, Budapest, Hungary
G. Bencze, C. Hajdu, D. Horvath[20], Á. Hunyadi, F. Sikler, T.Á. Vámi, V. Veszpremi, G. Vesztergombi[†]

Institute of Nuclear Research ATOMKI, Debrecen, Hungary
N. Beni, S. Czellar, J. Karancsi[19], A. Makovec, J. Molnar, Z. Szillasi

Institute of Physics, University of Debrecen, Debrecen, Hungary
P. Raics, Z.L. Trocsanyi, B. Ujvari

Indian Institute of Science (IISc), Bangalore, India
S. Choudhury, J.R. Komaragiri, P.C. Tiwari

National Institute of Science Education and Research, HBNI, Bhubaneswar, India
S. Bahinipati[22], C. Kar, P. Mal, K. Mandal, A. Nayak[23], D.K. Sahoo[22], S.K. Swain

Panjab University, Chandigarh, India
S. Bansal, S.B. Beri, V. Bhatnagar, S. Chauhan, R. Chawla, N. Dhingra, R. Gupta, A. Kaur, M. Kaur, S. Kaur, P. Kumari, M. Lohan, A. Mehta, K. Sandeep, S. Sharma, J.B. Singh, A.K. Virdi, G. Walia

JHEP04(2019)112

University of Delhi, Delhi, India

A. Bhardwaj, B.C. Choudhary, R.B. Garg, M. Gola, S. Keshri, Ashok Kumar, S. Malhotra, M. Naimuddin, P. Priyanka, K. Ranjan, Aashaq Shah, R. Sharma

Saha Institute of Nuclear Physics, HBNI, Kolkata, India

R. Bhardwaj[24], M. Bharti[24], R. Bhattacharya, S. Bhattacharya, U. Bhawandeep[24], D. Bhowmik, S. Dey, S. Dutt[24], S. Dutta, S. Ghosh, K. Mondal, S. Nandan, A. Purohit, P.K. Rout, A. Roy, S. Roy Chowdhury, G. Saha, S. Sarkar, M. Sharan, B. Singh[24], S. Thakur[24]

Indian Institute of Technology Madras, Madras, India

P.K. Behera

Bhabha Atomic Research Centre, Mumbai, India

R. Chudasama, D. Dutta, V. Jha, V. Kumar, P.K. Netrakanti, L.M. Pant, P. Shukla

Tata Institute of Fundamental Research-A, Mumbai, India

T. Aziz, M.A. Bhat, S. Dugad, G.B. Mohanty, N. Sur, B. Sutar, RavindraKumar Verma

Tata Institute of Fundamental Research-B, Mumbai, India

S. Banerjee, S. Bhattacharya, S. Chatterjee, P. Das, M. Guchait, Sa. Jain, S. Karmakar, S. Kumar, M. Maity[25], G. Majumder, K. Mazumdar, N. Sahoo, T. Sarkar[25]

Indian Institute of Science Education and Research (IISER), Pune, India

S. Chauhan, S. Dube, V. Hegde, A. Kapoor, K. Kothekar, S. Pandey, A. Rane, A. Rastogi, S. Sharma

Institute for Research in Fundamental Sciences (IPM), Tehran, Iran

S. Chenarani[26], E. Eskandari Tadavani, S.M. Etesami[26], M. Khakzad, M. Mohammadi Najafabadi, M. Naseri, F. Rezaei Hosseinabadi, B. Safarzadeh[27], M. Zeinali

University College Dublin, Dublin, Ireland

M. Felcini, M. Grunewald

INFN Sezione di Bari [a], Università di Bari [b], Politecnico di Bari [c], Bari, Italy

M. Abbrescia[a,b], C. Calabria[a,b], A. Colaleo[a], D. Creanza[a,c], L. Cristella[a,b], N. De Filippis[a,c], M. De Palma[a,b], A. Di Florio[a,b], F. Errico[a,b], L. Fiore[a], A. Gelmi[a,b], G. Iaselli[a,c], M. Ince[a,b], S. Lezki[a,b], G. Maggi[a,c], M. Maggi[a], G. Miniello[a,b], S. My[a,b], S. Nuzzo[a,b], A. Pompili[a,b], G. Pugliese[a,c], R. Radogna[a], A. Ranieri[a], G. Selvaggi[a,b], A. Sharma[a], L. Silvestris[a], R. Venditti[a], P. Verwilligen[a], G. Zito[a]

INFN Sezione di Bologna [a], Università di Bologna [b], Bologna, Italy

G. Abbiendi[a], C. Battilana[a,b], D. Bonacorsi[a,b], L. Borgonovi[a,b], S. Braibant-Giacomelli[a,b], R. Campanini[a,b], P. Capiluppi[a,b], A. Castro[a,b], F.R. Cavallo[a], S.S. Chhibra[a,b], C. Ciocca[a], G. Codispoti[a,b], M. Cuffiani[a,b], G.M. Dallavalle[a], F. Fabbri[a], A. Fanfani[a,b], E. Fontanesi, P. Giacomelli[a], C. Grandi[a], L. Guiducci[a,b], S. Lo Meo[a], S. Marcellini[a], G. Masetti[a], A. Montanari[a], F.L. Navarria[a,b], A. Perrotta[a], F. Primavera[a,b,15], A.M. Rossi[a,b], T. Rovelli[a,b], G.P. Siroli[a,b], N. Tosi[a]

JHEP04(2019)112

INFN Sezione di Catania [a], Università di Catania [b], Catania, Italy

S. Albergo[a,b], A. Di Mattia[a], R. Potenza[a,b], A. Tricomi[a,b], C. Tuve[a,b]

INFN Sezione di Firenze [a], Università di Firenze [b], Firenze, Italy

G. Barbagli[a], K. Chatterjee[a,b], V. Ciulli[a,b], C. Civinini[a], R. D'Alessandro[a,b], E. Focardi[a,b], G. Latino, P. Lenzi[a,b], M. Meschini[a], S. Paoletti[a], L. Russo[a,28], G. Sguazzoni[a], D. Strom[a], L. Viliani[a]

INFN Laboratori Nazionali di Frascati, Frascati, Italy

L. Benussi, S. Bianco, F. Fabbri, D. Piccolo

INFN Sezione di Genova [a], Università di Genova [b], Genova, Italy

F. Ferro[a], R. Mulargia[a,b], F. Ravera[a,b], E. Robutti[a], S. Tosi[a,b]

INFN Sezione di Milano-Bicocca [a], Università di Milano-Bicocca [b], Milano, Italy

A. Benaglia[a], A. Beschi[b], F. Brivio[a,b], V. Ciriolo[a,b,15], S. Di Guida[a,d,15], M.E. Dinardo[a,b], S. Fiorendi[a,b], S. Gennai[a], A. Ghezzi[a,b], P. Govoni[a,b], M. Malberti[a,b], S. Malvezzi[a], A. Massironi[a,b], D. Menasce[a], F. Monti, L. Moroni[a], M. Paganoni[a,b], D. Pedrini[a], S. Ragazzi[a,b], T. Tabarelli de Fatis[a,b], D. Zuolo[a,b]

INFN Sezione di Napoli [a], Università di Napoli 'Federico II' [b], Napoli, Italy, Università della Basilicata [c], Potenza, Italy, Università G. Marconi [d], Roma, Italy

S. Buontempo[a], N. Cavallo[a,c], A. De Iorio[a,b], A. Di Crescenzo[a,b], F. Fabozzi[a,c], F. Fienga[a], G. Galati[a], A.O.M. Iorio[a,b], W.A. Khan[a], L. Lista[a], S. Meola[a,d,15], P. Paolucci[a,15], C. Sciacca[a,b], E. Voevodina[a,b]

INFN Sezione di Padova [a], Università di Padova [b], Padova, Italy, Università di Trento [c], Trento, Italy

P. Azzi[a], N. Bacchetta[a], D. Bisello[a,b], A. Boletti[a,b], A. Bragagnolo, R. Carlin[a,b], P. Checchia[a], M. Dall'Osso[a,b], P. De Castro Manzano[a], T. Dorigo[a], F. Gasparini[a,b], U. Gasparini[a,b], A. Gozzelino[a], S.Y. Hoh, S. Lacaprara[a], P. Lujan, M. Margoni[a,b], A.T. Meneguzzo[a,b], J. Pazzini[a,b], N. Pozzobon[a,b], P. Ronchese[a,b], R. Rossin[a,b], F. Simonetto[a,b], A. Tiko, E. Torassa[a], M. Tosi[a,b], M. Zanetti[a,b], P. Zotto[a,b], G. Zumerle[a,b]

INFN Sezione di Pavia [a], Università di Pavia [b], Pavia, Italy

A. Braghieri[a], A. Magnani[a], P. Montagna[a,b], S.P. Ratti[a,b], V. Re[a], M. Ressegotti[a,b], C. Riccardi[a,b], P. Salvini[a], I. Vai[a,b], P. Vitulo[a,b]

INFN Sezione di Perugia [a], Università di Perugia [b], Perugia, Italy

M. Biasini[a,b], G.M. Bilei[a], C. Cecchi[a,b], D. Ciangottini[a,b], L. Fanò[a,b], P. Lariccia[a,b], R. Leonardi[a,b], E. Manoni[a], G. Mantovani[a,b], V. Mariani[a,b], M. Menichelli[a], A. Rossi[a,b], A. Santocchia[a,b], D. Spiga[a]

JHEP04(2019)112

INFN Sezione di Pisa [a], Università di Pisa [b], Scuola Normale Superiore di Pisa [c], Pisa, Italy

K. Androsov[a], P. Azzurri[a], G. Bagliesi[a], L. Bianchini[a], T. Boccali[a], L. Borrello, R. Castaldi[a], M.A. Ciocci[a,b], R. Dell'Orso[a], G. Fedi[a], F. Fiori[a,c], L. Giannini[a,c], A. Giassi[a], M.T. Grippo[a], F. Ligabue[a,c], E. Manca[a,c], G. Mandorli[a,c], A. Messineo[a,b], F. Palla[a], A. Rizzi[a,b], G. Rolandi[29], P. Spagnolo[a], R. Tenchini[a], G. Tonelli[a,b], A. Venturi[a], P.G. Verdini[a]

INFN Sezione di Roma [a], Sapienza Università di Roma [b], Rome, Italy

L. Barone[a,b], F. Cavallari[a], M. Cipriani[a,b], D. Del Re[a,b], E. Di Marco[a,b], M. Diemoz[a], S. Gelli[a,b], E. Longo[a,b], B. Marzocchi[a,b], P. Meridiani[a], G. Organtini[a,b], F. Pandolfi[a], R. Paramatti[a,b], F. Preiato[a,b], S. Rahatlou[a,b], C. Rovelli[a], F. Santanastasio[a,b]

INFN Sezione di Torino [a], Università di Torino [b], Torino, Italy, Università del Piemonte Orientale [c], Novara, Italy

N. Amapane[a,b], R. Arcidiacono[a,c], S. Argiro[a,b], M. Arneodo[a,c], N. Bartosik[a], R. Bellan[a,b], C. Biino[a], A. Cappati[a,b], N. Cartiglia[a], F. Cenna[a,b], S. Cometti[a], M. Costa[a,b], R. Covarelli[a,b], N. Demaria[a], B. Kiani[a,b], C. Mariotti[a], S. Maselli[a], E. Migliore[a,b], V. Monaco[a,b], E. Monteil[a,b], M. Monteno[a], M.M. Obertino[a,b], L. Pacher[a,b], N. Pastrone[a], M. Pelliccioni[a], G.L. Pinna Angioni[a,b], A. Romero[a,b], M. Ruspa[a,c], R. Sacchi[a,b], R. Salvatico[a,b], K. Shchelina[a,b], V. Sola[a], A. Solano[a,b], D. Soldi[a,b], A. Staiano[a]

INFN Sezione di Trieste [a], Università di Trieste [b], Trieste, Italy

S. Belforte[a], V. Candelise[a,b], M. Casarsa[a], F. Cossutti[a], A. Da Rold[a,b], G. Della Ricca[a,b], F. Vazzoler[a,b], A. Zanetti[a]

Kyungpook National University, Daegu, Korea

D.H. Kim, G.N. Kim, M.S. Kim, J. Lee, S. Lee, S.W. Lee, C.S. Moon, Y.D. Oh, S.I. Pak, S. Sekmen, D.C. Son, Y.C. Yang

Chonnam National University, Institute for Universe and Elementary Particles, Kwangju, Korea

H. Kim, D.H. Moon, G. Oh

Hanyang University, Seoul, Korea

B. Francois, J. Goh[30], T.J. Kim

Korea University, Seoul, Korea

S. Cho, S. Choi, Y. Go, D. Gyun, S. Ha, B. Hong, Y. Jo, K. Lee, K.S. Lee, S. Lee, J. Lim, S.K. Park, Y. Roh

Sejong University, Seoul, Korea

H.S. Kim

Seoul National University, Seoul, Korea

J. Almond, J. Kim, J.S. Kim, H. Lee, K. Lee, K. Nam, S.B. Oh, B.C. Radburn-Smith, S.h. Seo, U.K. Yang, H.D. Yoo, G.B. Yu

JHEP04(2019)112

University of Seoul, Seoul, Korea
D. Jeon, H. Kim, J.H. Kim, J.S.H. Lee, I.C. Park

Sungkyunkwan University, Suwon, Korea
Y. Choi, C. Hwang, J. Lee, I. Yu

Vilnius University, Vilnius, Lithuania
V. Dudenas, A. Juodagalvis, J. Vaitkus

National Centre for Particle Physics, Universiti Malaya, Kuala Lumpur, Malaysia
I. Ahmed, Z.A. Ibrahim, M.A.B. Md Ali[31], F. Mohamad Idris[32], W.A.T. Wan Abdullah, M.N. Yusli, Z. Zolkapli

Universidad de Sonora (UNISON), Hermosillo, Mexico
J.F. Benitez, A. Castaneda Hernandez, J.A. Murillo Quijada

Centro de Investigacion y de Estudios Avanzados del IPN, Mexico City, Mexico
H. Castilla-Valdez, E. De La Cruz-Burelo, M.C. Duran-Osuna, I. Heredia-De La Cruz[33], R. Lopez-Fernandez, J. Mejia Guisao, R.I. Rabadan-Trejo, M. Ramirez-Garcia, G. Ramirez-Sanchez, R. Reyes-Almanza, A. Sanchez-Hernandez

Universidad Iberoamericana, Mexico City, Mexico
S. Carrillo Moreno, C. Oropeza Barrera, F. Vazquez Valencia

Benemerita Universidad Autonoma de Puebla, Puebla, Mexico
J. Eysermans, I. Pedraza, H.A. Salazar Ibarguen, C. Uribe Estrada

Universidad Autónoma de San Luis Potosí, San Luis Potosí, Mexico
A. Morelos Pineda

University of Auckland, Auckland, New Zealand
D. Krofcheck

University of Canterbury, Christchurch, New Zealand
S. Bheesette, P.H. Butler

National Centre for Physics, Quaid-I-Azam University, Islamabad, Pakistan
A. Ahmad, M. Ahmad, M.I. Asghar, Q. Hassan, H.R. Hoorani, A. Saddique, M.A. Shah, M. Shoaib, M. Waqas

National Centre for Nuclear Research, Swierk, Poland
H. Bialkowska, M. Bluj, B. Boimska, T. Frueboes, M. Górski, M. Kazana, M. Szleper, P. Traczyk, P. Zalewski

Institute of Experimental Physics, Faculty of Physics, University of Warsaw, Warsaw, Poland
K. Bunkowski, A. Byszuk[34], K. Doroba, A. Kalinowski, M. Konecki, J. Krolikowski, M. Misiura, M. Olszewski, A. Pyskir, M. Walczak

JHEP04(2019)112

Laboratório de Instrumentação e Física Experimental de Partículas, Lisboa, Portugal

M. Araujo, P. Bargassa, C. Beirão Da Cruz E Silva, A. Di Francesco, P. Faccioli, B. Galinhas, M. Gallinaro, J. Hollar, N. Leonardo, J. Seixas, G. Strong, O. Toldaiev, J. Varela

Joint Institute for Nuclear Research, Dubna, Russia

S. Afanasiev, P. Bunin, M. Gavrilenko, I. Golutvin, I. Gorbunov, A. Kamenev, V. Karjavine, A. Lanev, A. Malakhov, V. Matveev[35,36], P. Moisenz, V. Palichik, V. Perelygin, S. Shmatov, S. Shulha, N. Skatchkov, V. Smirnov, N. Voytishin, A. Zarubin

Petersburg Nuclear Physics Institute, Gatchina (St. Petersburg), Russia

V. Golovtsov, Y. Ivanov, V. Kim[37], E. Kuznetsova[38], P. Levchenko, V. Murzin, V. Oreshkin, I. Smirnov, D. Sosnov, V. Sulimov, L. Uvarov, S. Vavilov, A. Vorobyev

Institute for Nuclear Research, Moscow, Russia

Yu. Andreev, A. Dermenev, S. Gninenko, N. Golubev, A. Karneyeu, M. Kirsanov, N. Krasnikov, A. Pashenkov, D. Tlisov, A. Toropin

Institute for Theoretical and Experimental Physics, Moscow, Russia

V. Epshteyn, V. Gavrilov, N. Lychkovskaya, V. Popov, I. Pozdnyakov, G. Safronov, A. Spiridonov, A. Stepennov, V. Stolin, M. Toms, E. Vlasov, A. Zhokin

Moscow Institute of Physics and Technology, Moscow, Russia

T. Aushev

National Research Nuclear University 'Moscow Engineering Physics Institute' (MEPhI), Moscow, Russia

R. Chistov[39], M. Danilov[39], P. Parygin, D. Philippov, S. Polikarpov[39], E. Tarkovskii

P.N. Lebedev Physical Institute, Moscow, Russia

V. Andreev, M. Azarkin, I. Dremin[36], M. Kirakosyan, A. Terkulov

Skobeltsyn Institute of Nuclear Physics, Lomonosov Moscow State University, Moscow, Russia

A. Baskakov, A. Belyaev, E. Boos, V. Bunichev, M. Dubinin[40], L. Dudko, A. Gribushin, V. Klyukhin, O. Kodolova, I. Lokhtin, I. Miagkov, S. Obraztsov, S. Petrushanko, V. Savrin, A. Snigirev

Novosibirsk State University (NSU), Novosibirsk, Russia

A. Barnyakov[41], V. Blinov[41], T. Dimova[41], L. Kardapoltsev[41], Y. Skovpen[41]

Institute for High Energy Physics of National Research Centre 'Kurchatov Institute', Protvino, Russia

I. Azhgirey, I. Bayshev, S. Bitioukov, D. Elumakhov, A. Godizov, V. Kachanov, A. Kalinin, D. Konstantinov, P. Mandrik, V. Petrov, R. Ryutin, S. Slabospitskii, A. Sobol, S. Troshin, N. Tyurin, A. Uzunian, A. Volkov

JHEP04(2019)112

National Research Tomsk Polytechnic University, Tomsk, Russia
A. Babaev, S. Baidali, V. Okhotnikov

University of Belgrade, Faculty of Physics and Vinca Institute of Nuclear Sciences, Belgrade, Serbia
P. Adzic[42], P. Cirkovic, D. Devetak, M. Dordevic, J. Milosevic

Centro de Investigaciones Energéticas Medioambientales y Tecnológicas (CIEMAT), Madrid, Spain
J. Alcaraz Maestre, A. Álvarez Fernández, I. Bachiller, M. Barrio Luna, J.A. Brochero Cifuentes, M. Cerrada, N. Colino, B. De La Cruz, A. Delgado Peris, C. Fernandez Bedoya, J.P. Fernández Ramos, J. Flix, M.C. Fouz, O. Gonzalez Lopez, S. Goy Lopez, J.M. Hernandez, M.I. Josa, D. Moran, A. Pérez-Calero Yzquierdo, J. Puerta Pelayo, I. Redondo, L. Romero, M.S. Soares, A. Triossi

Universidad Autónoma de Madrid, Madrid, Spain
C. Albajar, J.F. de Trocóniz

Universidad de Oviedo, Oviedo, Spain
J. Cuevas, C. Erice, J. Fernandez Menendez, S. Folgueras, I. Gonzalez Caballero, J.R. González Fernández, E. Palencia Cortezon, V. Rodríguez Bouza, S. Sanchez Cruz, P. Vischia, J.M. Vizan Garcia

Instituto de Física de Cantabria (IFCA), CSIC-Universidad de Cantabria, Santander, Spain
I.J. Cabrillo, A. Calderon, B. Chazin Quero, J. Duarte Campderros, M. Fernandez, P.J. Fernández Manteca, A. García Alonso, J. Garcia-Ferrero, G. Gomez, A. Lopez Virto, J. Marco, C. Martinez Rivero, P. Martinez Ruiz del Arbol, F. Matorras, J. Piedra Gomez, C. Prieels, T. Rodrigo, A. Ruiz-Jimeno, L. Scodellaro, N. Trevisani, I. Vila, R. Vilar Cortabitarte

University of Ruhuna, Department of Physics, Matara, Sri Lanka
N. Wickramage

CERN, European Organization for Nuclear Research, Geneva, Switzerland
D. Abbaneo, B. Akgun, E. Auffray, G. Auzinger, P. Baillon, A.H. Ball, D. Barney, J. Bendavid, M. Bianco, A. Bocci, C. Botta, E. Brondolin, T. Camporesi, M. Cepeda, G. Cerminara, E. Chapon, Y. Chen, G. Cucciati, D. d'Enterria, A. Dabrowski, N. Daci, V. Daponte, A. David, A. De Roeck, N. Deelen, M. Dobson, M. Dünser, N. Dupont, A. Elliott-Peisert, P. Everaerts, F. Fallavollita[43], D. Fasanella, G. Franzoni, J. Fulcher, W. Funk, D. Gigi, A. Gilbert, K. Gill, F. Glege, M. Gruchala, M. Guilbaud, D. Gulhan, J. Hegeman, C. Heidegger, V. Innocente, A. Jafari, P. Janot, O. Karacheban[18], J. Kieseler, A. Kornmayer, M. Krammer[1], C. Lange, P. Lecoq, C. Lourenço, L. Malgeri, M. Mannelli, F. Meijers, J.A. Merlin, S. Mersi, E. Meschi, P. Milenovic[44], F. Moortgat, M. Mulders, J. Ngadiuba, S. Nourbakhsh, S. Orfanelli, L. Orsini, F. Pantaleo[15], L. Pape, E. Perez, M. Peruzzi, A. Petrilli, G. Petrucciani, A. Pfeiffer, M. Pierini, F.M. Pitters, D. Rabady, A. Racz, T. Reis, M. Rovere, H. Sakulin, C. Schäfer, C. Schwick, M. Seidel, M. Selvaggi,

JHEP04(2019)112

A. Sharma, P. Silva, P. Sphicas[45], A. Stakia, J. Steggemann, D. Treille, A. Tsirou, V. Veckalns[46], M. Verzetti, W.D. Zeuner

Paul Scherrer Institut, Villigen, Switzerland

L. Caminada[47], K. Deiters, W. Erdmann, R. Horisberger, Q. Ingram, H.C. Kaestli, D. Kotlinski, U. Langenegger, T. Rohe, S.A. Wiederkehr

ETH Zurich - Institute for Particle Physics and Astrophysics (IPA), Zurich, Switzerland

M. Backhaus, L. Bäni, P. Berger, N. Chernyavskaya, G. Dissertori, M. Dittmar, M. Donegà, C. Dorfer, T.A. Gómez Espinosa, C. Grab, D. Hits, T. Klijnsma, W. Lustermann, R.A. Manzoni, M. Marionneau, M.T. Meinhard, F. Micheli, P. Musella, F. Nessi-Tedaldi, J. Pata, F. Pauss, G. Perrin, L. Perrozzi, S. Pigazzini, M. Quittnat, C. Reissel, D. Ruini, D.A. Sanz Becerra, M. Schönenberger, L. Shchutska, V.R. Tavolaro, K. Theofilatos, M.L. Vesterbacka Olsson, R. Wallny, D.H. Zhu

Universität Zürich, Zurich, Switzerland

T.K. Aarrestad, C. Amsler[48], D. Brzhechko, M.F. Canelli, A. De Cosa, R. Del Burgo, S. Donato, C. Galloni, T. Hreus, B. Kilminster, S. Leontsinis, I. Neutelings, G. Rauco, P. Robmann, D. Salerno, K. Schweiger, C. Seitz, Y. Takahashi, A. Zucchetta

National Central University, Chung-Li, Taiwan

T.H. Doan, R. Khurana, C.M. Kuo, W. Lin, A. Pozdnyakov, S.S. Yu

National Taiwan University (NTU), Taipei, Taiwan

P. Chang, Y. Chao, K.F. Chen, P.H. Chen, W.-S. Hou, Arun Kumar, Y.F. Liu, R.-S. Lu, E. Paganis, A. Psallidas, A. Steen

Chulalongkorn University, Faculty of Science, Department of Physics, Bangkok, Thailand

B. Asavapibhop, N. Srimanobhas, N. Suwonjandee

Çukurova University, Physics Department, Science and Art Faculty, Adana, Turkey

M.N. Bakirci[49], A. Bat, F. Boran, S. Cerci[50], S. Damarseckin, Z.S. Demiroglu, F. Dolek, C. Dozen, I. Dumanoglu, E. Eskut, S. Girgis, G. Gokbulut, Y. Guler, E. Gurpinar, I. Hos[51], C. Isik, E.E. Kangal[52], O. Kara, A. Kayis Topaksu, U. Kiminsu, M. Oglakci, G. Onengut, K. Ozdemir[53], A. Polatoz, U.G. Tok, S. Turkcapar, I.S. Zorbakir, C. Zorbilmez

Middle East Technical University, Physics Department, Ankara, Turkey

B. Isildak[54], G. Karapinar[55], M. Yalvac, M. Zeyrek

Bogazici University, Istanbul, Turkey

I.O. Atakisi, E. Gülmez, M. Kaya[56], O. Kaya[57], S. Ozkorucuklu[58], S. Tekten, E.A. Yetkin[59]

Istanbul Technical University, Istanbul, Turkey

M.N. Agaras, A. Cakir, K. Cankocak, Y. Komurcu, S. Sen[60]

JHEP04(2019)112

Institute for Scintillation Materials of National Academy of Science of Ukraine, Kharkov, Ukraine

B. Grynyov

National Scientific Center, Kharkov Institute of Physics and Technology, Kharkov, Ukraine

L. Levchuk

University of Bristol, Bristol, United Kingdom

F. Ball, J.J. Brooke, D. Burns, E. Clement, D. Cussans, O. Davignon, H. Flacher, J. Goldstein, G.P. Heath, H.F. Heath, L. Kreczko, D.M. Newbold[61], S. Paramesvaran, B. Penning, T. Sakuma, D. Smith, V.J. Smith, J. Taylor, A. Titterton

Rutherford Appleton Laboratory, Didcot, United Kingdom

K.W. Bell, A. Belyaev[62], C. Brew, R.M. Brown, D. Cieri, D.J.A. Cockerill, J.A. Coughlan, K. Harder, S. Harper, J. Linacre, E. Olaiya, D. Petyt, C.H. Shepherd-Themistocleous, A. Thea, I.R. Tomalin, T. Williams, W.J. Womersley

Imperial College, London, United Kingdom

R. Bainbridge, P. Bloch, J. Borg, S. Breeze, O. Buchmuller, A. Bundock, D. Colling, P. Dauncey, G. Davies, M. Della Negra, R. Di Maria, G. Hall, G. Iles, T. James, M. Komm, C. Laner, L. Lyons, A.-M. Magnan, S. Malik, A. Martelli, J. Nash[63], A. Nikitenko[7], V. Palladino, M. Pesaresi, D.M. Raymond, A. Richards, A. Rose, E. Scott, C. Seez, A. Shtipliyski, G. Singh, M. Stoye, T. Strebler, S. Summers, A. Tapper, K. Uchida, T. Virdee[15], N. Wardle, D. Winterbottom, J. Wright, S.C. Zenz

Brunel University, Uxbridge, United Kingdom

J.E. Cole, P.R. Hobson, A. Khan, P. Kyberd, C.K. Mackay, A. Morton, I.D. Reid, L. Teodorescu, S. Zahid

Baylor University, Waco, U.S.A.

K. Call, J. Dittmann, K. Hatakeyama, H. Liu, C. Madrid, B. McMaster, N. Pastika, C. Smith

Catholic University of America, Washington DC, U.S.A.

R. Bartek, A. Dominguez

The University of Alabama, Tuscaloosa, U.S.A.

A. Buccilli, S.I. Cooper, C. Henderson, P. Rumerio, C. West

Boston University, Boston, U.S.A.

D. Arcaro, T. Bose, D. Gastler, D. Pinna, D. Rankin, C. Richardson, J. Rohlf, L. Sulak, D. Zou

Brown University, Providence, U.S.A.

G. Benelli, X. Coubez, D. Cutts, M. Hadley, J. Hakala, U. Heintz, J.M. Hogan[64], K.H.M. Kwok, E. Laird, G. Landsberg, J. Lee, Z. Mao, M. Narain, S. Sagir[65], R. Syarif, E. Usai, D. Yu

JHEP04(2019)112

University of California, Davis, Davis, U.S.A.

R. Band, C. Brainerd, R. Breedon, D. Burns, M. Calderon De La Barca Sanchez, M. Chertok, J. Conway, R. Conway, P.T. Cox, R. Erbacher, C. Flores, G. Funk, W. Ko, O. Kukral, R. Lander, M. Mulhearn, D. Pellett, J. Pilot, S. Shalhout, M. Shi, D. Stolp, D. Taylor, K. Tos, M. Tripathi, Z. Wang, F. Zhang

University of California, Los Angeles, U.S.A.

M. Bachtis, C. Bravo, R. Cousins, A. Dasgupta, A. Florent, J. Hauser, M. Ignatenko, N. Mccoll, S. Regnard, D. Saltzberg, C. Schnaible, V. Valuev

University of California, Riverside, Riverside, U.S.A.

E. Bouvier, K. Burt, R. Clare, J.W. Gary, S.M.A. Ghiasi Shirazi, G. Hanson, G. Karapostoli, E. Kennedy, F. Lacroix, O.R. Long, M. Olmedo Negrete, M.I. Paneva, W. Si, L. Wang, H. Wei, S. Wimpenny, B.R. Yates

University of California, San Diego, La Jolla, U.S.A.

J.G. Branson, P. Chang, S. Cittolin, M. Derdzinski, R. Gerosa, D. Gilbert, B. Hashemi, A. Holzner, D. Klein, G. Kole, V. Krutelyov, J. Letts, M. Masciovecchio, D. Olivito, S. Padhi, M. Pieri, M. Sani, V. Sharma, S. Simon, M. Tadel, A. Vartak, S. Wasserbaech[66], J. Wood, F. Würthwein, A. Yagil, G. Zevi Della Porta

University of California, Santa Barbara - Department of Physics, Santa Barbara, U.S.A.

N. Amin, R. Bhandari, C. Campagnari, M. Citron, V. Dutta, M. Franco Sevilla, L. Gouskos, R. Heller, J. Incandela, A. Ovcharova, H. Qu, J. Richman, D. Stuart, I. Suarez, S. Wang, J. Yoo

California Institute of Technology, Pasadena, U.S.A.

D. Anderson, A. Bornheim, J.M. Lawhorn, N. Lu, H.B. Newman, T.Q. Nguyen, M. Spiropulu, J.R. Vlimant, R. Wilkinson, S. Xie, Z. Zhang, R.Y. Zhu

Carnegie Mellon University, Pittsburgh, U.S.A.

M.B. Andrews, T. Ferguson, T. Mudholkar, M. Paulini, M. Sun, I. Vorobiev, M. Weinberg

University of Colorado Boulder, Boulder, U.S.A.

J.P. Cumalat, W.T. Ford, F. Jensen, A. Johnson, E. MacDonald, T. Mulholland, R. Patel, A. Perloff, K. Stenson, K.A. Ulmer, S.R. Wagner

Cornell University, Ithaca, U.S.A.

J. Alexander, J. Chaves, Y. Cheng, J. Chu, A. Datta, K. Mcdermott, N. Mirman, J.R. Patterson, D. Quach, A. Rinkevicius, A. Ryd, L. Skinnari, L. Soffi, S.M. Tan, Z. Tao, J. Thom, J. Tucker, P. Wittich, M. Zientek

Fermi National Accelerator Laboratory, Batavia, U.S.A.

S. Abdullin, M. Albrow, M. Alyari, G. Apollinari, A. Apresyan, A. Apyan, S. Banerjee, L.A.T. Bauerdick, A. Beretvas, J. Berryhill, P.C. Bhat, K. Burkett, J.N. Butler, A. Canepa, G.B. Cerati, H.W.K. Cheung, F. Chlebana, M. Cremonesi, J. Duarte, V.D. Elvira, J. Freeman, Z. Gecse, E. Gottschalk, L. Gray, D. Green, S. Grünendahl, O. Gutsche,

JHEP04(2019)112

J. Hanlon, R.M. Harris, S. Hasegawa, J. Hirschauer, Z. Hu, B. Jayatilaka, S. Jindariani, M. Johnson, U. Joshi, B. Klima, M.J. Kortelainen, B. Kreis, S. Lammel, D. Lincoln, R. Lipton, M. Liu, T. Liu, J. Lykken, K. Maeshima, J.M. Marraffino, D. Mason, P. McBride, P. Merkel, S. Mrenna, S. Nahn, V. O'Dell, K. Pedro, C. Pena, O. Prokofyev, G. Rakness, L. Ristori, A. Savoy-Navarro[67], B. Schneider, E. Sexton-Kennedy, A. Soha, W.J. Spalding, L. Spiegel, S. Stoynev, J. Strait, N. Strobbe, L. Taylor, S. Tkaczyk, N.V. Tran, L. Uplegger, E.W. Vaandering, C. Vernieri, M. Verzocchi, R. Vidal, M. Wang, H.A. Weber, A. Whitbeck

University of Florida, Gainesville, U.S.A.

D. Acosta, P. Avery, P. Bortignon, D. Bourilkov, A. Brinkerhoff, L. Cadamuro, A. Carnes, D. Curry, R.D. Field, S.V. Gleyzer, B.M. Joshi, J. Konigsberg, A. Korytov, K.H. Lo, P. Ma, K. Matchev, H. Mei, G. Mitselmakher, D. Rosenzweig, K. Shi, D. Sperka, J. Wang, S. Wang, X. Zuo

Florida International University, Miami, U.S.A.

Y.R. Joshi, S. Linn

Florida State University, Tallahassee, U.S.A.

A. Ackert, T. Adams, A. Askew, S. Hagopian, V. Hagopian, K.F. Johnson, T. Kolberg, G. Martinez, T. Perry, H. Prosper, A. Saha, C. Schiber, R. Yohay

Florida Institute of Technology, Melbourne, U.S.A.

M.M. Baarmand, V. Bhopatkar, S. Colafranceschi, M. Hohlmann, D. Noonan, M. Rahmani, T. Roy, F. Yumiceva

University of Illinois at Chicago (UIC), Chicago, U.S.A.

M.R. Adams, L. Apanasevich, D. Berry, R.R. Betts, R. Cavanaugh, X. Chen, S. Dittmer, O. Evdokimov, C.E. Gerber, D.A. Hangal, D.J. Hofman, K. Jung, J. Kamin, C. Mills, M.B. Tonjes, N. Varelas, H. Wang, X. Wang, Z. Wu, J. Zhang

The University of Iowa, Iowa City, U.S.A.

M. Alhusseini, B. Bilki[68], W. Clarida, K. Dilsiz[69], S. Durgut, R.P. Gandrajula, M. Haytmyradov, V. Khristenko, J.-P. Merlo, A. Mestvirishvili, A. Moeller, J. Nachtman, H. Ogul[70], Y. Onel, F. Ozok[71], A. Penzo, C. Snyder, E. Tiras, J. Wetzel

Johns Hopkins University, Baltimore, U.S.A.

B. Blumenfeld, A. Cocoros, N. Eminizer, D. Fehling, L. Feng, A.V. Gritsan, W.T. Hung, P. Maksimovic, J. Roskes, U. Sarica, M. Swartz, M. Xiao, C. You

The University of Kansas, Lawrence, U.S.A.

A. Al-bataineh, P. Baringer, A. Bean, S. Boren, J. Bowen, A. Bylinkin, J. Castle, S. Khalil, A. Kropivnitskaya, D. Majumder, W. Mcbrayer, M. Murray, C. Rogan, S. Sanders, E. Schmitz, J.D. Tapia Takaki, Q. Wang

Kansas State University, Manhattan, U.S.A.

S. Duric, A. Ivanov, K. Kaadze, D. Kim, Y. Maravin, D.R. Mendis, T. Mitchell, A. Modak, A. Mohammadi, L.K. Saini

JHEP04(2019)112

Lawrence Livermore National Laboratory, Livermore, U.S.A.

F. Rebassoo, D. Wright

University of Maryland, College Park, U.S.A.

A. Baden, O. Baron, A. Belloni, S.C. Eno, Y. Feng, C. Ferraioli, N.J. Hadley, S. Jabeen, G.Y. Jeng, R.G. Kellogg, J. Kunkle, A.C. Mignerey, S. Nabili, F. Ricci-Tam, Y.H. Shin, A. Skuja, S.C. Tonwar, K. Wong

Massachusetts Institute of Technology, Cambridge, U.S.A.

D. Abercrombie, B. Allen, V. Azzolini, A. Baty, G. Bauer, R. Bi, S. Brandt, W. Busza, I.A. Cali, M. D'Alfonso, Z. Demiragli, G. Gomez Ceballos, M. Goncharov, P. Harris, D. Hsu, M. Hu, Y. Iiyama, G.M. Innocenti, M. Klute, D. Kovalskyi, Y.-J. Lee, P.D. Luckey, B. Maier, A.C. Marini, C. Mcginn, C. Mironov, S. Narayanan, X. Niu, C. Paus, C. Roland, G. Roland, Z. Shi, G.S.F. Stephans, K. Sumorok, K. Tatar, D. Velicanu, J. Wang, T.W. Wang, B. Wyslouch

University of Minnesota, Minneapolis, U.S.A.

A.C. Benvenuti[†], R.M. Chatterjee, A. Evans, P. Hansen, J. Hiltbrand, Sh. Jain, S. Kalafut, M. Krohn, Y. Kubota, Z. Lesko, J. Mans, N. Ruckstuhl, R. Rusack, M.A. Wadud

University of Mississippi, Oxford, U.S.A.

J.G. Acosta, S. Oliveros

University of Nebraska-Lincoln, Lincoln, U.S.A.

E. Avdeeva, K. Bloom, D.R. Claes, C. Fangmeier, F. Golf, R. Gonzalez Suarez, R. Kamalieddin, I. Kravchenko, J. Monroy, J.E. Siado, G.R. Snow, B. Stieger

State University of New York at Buffalo, Buffalo, U.S.A.

A. Godshalk, C. Harrington, I. Iashvili, A. Kharchilava, C. Mclean, D. Nguyen, A. Parker, S. Rappoccio, B. Roozbahani

Northeastern University, Boston, U.S.A.

G. Alverson, E. Barberis, C. Freer, Y. Haddad, A. Hortiangtham, D.M. Morse, T. Orimoto, R. Teixeira De Lima, T. Wamorkar, B. Wang, A. Wisecarver, D. Wood

Northwestern University, Evanston, U.S.A.

S. Bhattacharya, J. Bueghly, O. Charaf, K.A. Hahn, N. Mucia, N. Odell, M.H. Schmitt, K. Sung, M. Trovato, M. Velasco

University of Notre Dame, Notre Dame, U.S.A.

R. Bucci, N. Dev, M. Hildreth, K. Hurtado Anampa, C. Jessop, D.J. Karmgard, N. Kellams, K. Lannon, W. Li, N. Loukas, N. Marinelli, F. Meng, C. Mueller, Y. Musienko[35], M. Planer, A. Reinsvold, R. Ruchti, P. Siddireddy, G. Smith, S. Taroni, M. Wayne, A. Wightman, M. Wolf, A. Woodard

The Ohio State University, Columbus, U.S.A.

J. Alimena, L. Antonelli, B. Bylsma, L.S. Durkin, S. Flowers, B. Francis, C. Hill, W. Ji, T.Y. Ling, W. Luo, B.L. Winer

JHEP04(2019)112

Princeton University, Princeton, U.S.A.

S. Cooperstein, P. Elmer, J. Hardenbrook, S. Higginbotham, A. Kalogeropoulos, D. Lange, M.T. Lucchini, J. Luo, D. Marlow, K. Mei, I. Ojalvo, J. Olsen, C. Palmer, P. Piroué, J. Salfeld-Nebgen, D. Stickland, C. Tully, Z. Wang

University of Puerto Rico, Mayaguez, U.S.A.

S. Malik, S. Norberg

Purdue University, West Lafayette, U.S.A.

A. Barker, V.E. Barnes, S. Das, L. Gutay, M. Jones, A.W. Jung, A. Khatiwada, B. Mahakud, D.H. Miller, N. Neumeister, C.C. Peng, S. Piperov, H. Qiu, J.F. Schulte, J. Sun, F. Wang, R. Xiao, W. Xie

Purdue University Northwest, Hammond, U.S.A.

T. Cheng, J. Dolen, N. Parashar

Rice University, Houston, U.S.A.

Z. Chen, K.M. Ecklund, S. Freed, F.J.M. Geurts, M. Kilpatrick, W. Li, B.P. Padley, R. Redjimi, J. Roberts, J. Rorie, W. Shi, Z. Tu, A. Zhang

University of Rochester, Rochester, U.S.A.

A. Bodek, P. de Barbaro, R. Demina, Y.t. Duh, J.L. Dulemba, C. Fallon, T. Ferbel, M. Galanti, A. Garcia-Bellido, J. Han, O. Hindrichs, A. Khukhunaishvili, E. Ranken, P. Tan, R. Taus

Rutgers, The State University of New Jersey, Piscataway, U.S.A.

A. Agapitos, J.P. Chou, Y. Gershtein, E. Halkiadakis, A. Hart, M. Heindl, E. Hughes, S. Kaplan, R. Kunnawalkam Elayavalli, S. Kyriacou, A. Lath, R. Montalvo, K. Nash, M. Osherson, H. Saka, S. Salur, S. Schnetzer, D. Sheffield, S. Somalwar, R. Stone, S. Thomas, P. Thomassen, M. Walker

University of Tennessee, Knoxville, U.S.A.

A.G. Delannoy, J. Heideman, G. Riley, S. Spanier

Texas A&M University, College Station, U.S.A.

O. Bouhali[72], A. Celik, M. Dalchenko, M. De Mattia, A. Delgado, S. Dildick, R. Eusebi, J. Gilmore, T. Huang, T. Kamon[73], S. Luo, R. Mueller, D. Overton, L. Perniè, D. Rathjens, A. Safonov

Texas Tech University, Lubbock, U.S.A.

N. Akchurin, J. Damgov, F. De Guio, P.R. Dudero, S. Kunori, K. Lamichhane, S.W. Lee, T. Mengke, S. Muthumuni, T. Peltola, S. Undleeb, I. Volobouev, Z. Wang

Vanderbilt University, Nashville, U.S.A.

S. Greene, A. Gurrola, R. Janjam, W. Johns, C. Maguire, A. Melo, H. Ni, K. Padeken, J.D. Ruiz Alvarez, P. Sheldon, S. Tuo, J. Velkovska, M. Verweij, Q. Xu

JHEP04(2019)112

University of Virginia, Charlottesville, U.S.A.

M.W. Arenton, P. Barria, B. Cox, R. Hirosky, M. Joyce, A. Ledovskoy, H. Li, C. Neu, T. Sinthuprasith, Y. Wang, E. Wolfe, F. Xia

Wayne State University, Detroit, U.S.A.

R. Harr, P.E. Karchin, N. Poudyal, J. Sturdy, P. Thapa, S. Zaleski

University of Wisconsin - Madison, Madison, WI, U.S.A.

M. Brodski, J. Buchanan, C. Caillol, D. Carlsmith, S. Dasu, I. De Bruyn, L. Dodd, B. Gomber, M. Grothe, M. Herndon, A. Hervé, U. Hussain, P. Klabbers, A. Lanaro, K. Long, R. Loveless, T. Ruggles, A. Savin, V. Sharma, N. Smith, W.H. Smith, N. Woods

†: Deceased
1: Also at Vienna University of Technology, Vienna, Austria
2: Also at IRFU, CEA, Université Paris-Saclay, Gif-sur-Yvette, France
3: Also at Universidade Estadual de Campinas, Campinas, Brazil
4: Also at Federal University of Rio Grande do Sul, Porto Alegre, Brazil
5: Also at Université Libre de Bruxelles, Bruxelles, Belgium
6: Also at University of Chinese Academy of Sciences, Beijing, China
7: Also at Institute for Theoretical and Experimental Physics, Moscow, Russia
8: Also at Joint Institute for Nuclear Research, Dubna, Russia
9: Also at Cairo University, Cairo, Egypt
10: Also at Helwan University, Cairo, Egypt
11: Now at Zewail City of Science and Technology, Zewail, Egypt
12: Also at Department of Physics, King Abdulaziz University, Jeddah, Saudi Arabia
13: Also at Université de Haute Alsace, Mulhouse, France
14: Also at Skobeltsyn Institute of Nuclear Physics, Lomonosov Moscow State University, Moscow, Russia
15: Also at CERN, European Organization for Nuclear Research, Geneva, Switzerland
16: Also at RWTH Aachen University, III. Physikalisches Institut A, Aachen, Germany
17: Also at University of Hamburg, Hamburg, Germany
18: Also at Brandenburg University of Technology, Cottbus, Germany
19: Also at Institute of Physics, University of Debrecen, Debrecen, Hungary
20: Also at Institute of Nuclear Research ATOMKI, Debrecen, Hungary
21: Also at MTA-ELTE Lendület CMS Particle and Nuclear Physics Group, Eötvös Loránd University, Budapest, Hungary
22: Also at Indian Institute of Technology Bhubaneswar, Bhubaneswar, India
23: Also at Institute of Physics, Bhubaneswar, India
24: Also at Shoolini University, Solan, India
25: Also at University of Visva-Bharati, Santiniketan, India
26: Also at Isfahan University of Technology, Isfahan, Iran
27: Also at Plasma Physics Research Center, Science and Research Branch, Islamic Azad University, Tehran, Iran
28: Also at Università degli Studi di Siena, Siena, Italy
29: Also at Scuola Normale e Sezione dell'INFN, Pisa, Italy
30: Also at Kyunghee University, Seoul, Korea
31: Also at International Islamic University of Malaysia, Kuala Lumpur, Malaysia
32: Also at Malaysian Nuclear Agency, MOSTI, Kajang, Malaysia

JHEP04(2019)112

33: Also at Consejo Nacional de Ciencia y Tecnología, Mexico city, Mexico
34: Also at Warsaw University of Technology, Institute of Electronic Systems, Warsaw, Poland
35: Also at Institute for Nuclear Research, Moscow, Russia
36: Now at National Research Nuclear University 'Moscow Engineering Physics Institute' (MEPhI), Moscow, Russia
37: Also at St. Petersburg State Polytechnical University, St. Petersburg, Russia
38: Also at University of Florida, Gainesville, U.S.A.
39: Also at P.N. Lebedev Physical Institute, Moscow, Russia
40: Also at California Institute of Technology, Pasadena, U.S.A.
41: Also at Budker Institute of Nuclear Physics, Novosibirsk, Russia
42: Also at Faculty of Physics, University of Belgrade, Belgrade, Serbia
43: Also at INFN Sezione di Pavia [a], Università di Pavia [b], Pavia, Italy
44: Also at University of Belgrade, Faculty of Physics and Vinca Institute of Nuclear Sciences, Belgrade, Serbia
45: Also at National and Kapodistrian University of Athens, Athens, Greece
46: Also at Riga Technical University, Riga, Latvia
47: Also at Universität Zürich, Zurich, Switzerland
48: Also at Stefan Meyer Institute for Subatomic Physics (SMI), Vienna, Austria
49: Also at Gaziosmanpasa University, Tokat, Turkey
50: Also at Adiyaman University, Adiyaman, Turkey
51: Also at Istanbul Aydin University, Istanbul, Turkey
52: Also at Mersin University, Mersin, Turkey
53: Also at Piri Reis University, Istanbul, Turkey
54: Also at Ozyegin University, Istanbul, Turkey
55: Also at Izmir Institute of Technology, Izmir, Turkey
56: Also at Marmara University, Istanbul, Turkey
57: Also at Kafkas University, Kars, Turkey
58: Also at Istanbul University, Faculty of Science, Istanbul, Turkey
59: Also at Istanbul Bilgi University, Istanbul, Turkey
60: Also at Hacettepe University, Ankara, Turkey
61: Also at Rutherford Appleton Laboratory, Didcot, United Kingdom
62: Also at School of Physics and Astronomy, University of Southampton, Southampton, United Kingdom
63: Also at Monash University, Faculty of Science, Clayton, Australia
64: Also at Bethel University, St. Paul, U.S.A.
65: Also at Karamanoğlu Mehmetbey University, Karaman, Turkey
66: Also at Utah Valley University, Orem, U.S.A.
67: Also at Purdue University, West Lafayette, U.S.A.
68: Also at Beykent University, Istanbul, Turkey
69: Also at Bingol University, Bingol, Turkey
70: Also at Sinop University, Sinop, Turkey
71: Also at Mimar Sinan University, Istanbul, Istanbul, Turkey
72: Also at Texas A&M University at Qatar, Doha, Qatar
73: Also at Kyungpook National University, Daegu, Korea

JHEP04(2019)112